RRS *JAMES CLARK ROSS*

VOYAGE 4

13 NOV 1994 - 12 DEC 1994

WOCE SR1 IN DRAKE PASSAGE

Stuart A. Cunningham

Steven G. Alderson

Draft Version 5

August 14, 1996

1. MEASUREMENT TECHNIQUES AND CALIBRATIONS

During Voyage 4 (R94) of the RRS James Clark Ross across the Drake Passage the WOCE Section SR1 was occupied. Full depth CTD stations were taken across the section and currents measured using a ship mounted ADCP, Table 0.

1.1 Salinity Sample Measurements

Salinity samples were analysed using the IOSDL Guildline Autosal model 8400B. This Autosal was modified by the addition of an Ocean Scientific International (OSI) peristaltic salinometer pump (Pump S/N 1007134 purchased August 1993). The pump was fitted according to instructions supplied by OSI. The pump was set to speed setting two ($\equiv$25 ml/min nominal) and was switched via an in line toggle switch, rather than through the flow speed switch.

The Autosal was observed to have a *zero* reading of + 6. The manual suggests that a reading within ± 5 is appropriate for a "within calibration" Autosal. The + 6 *zero* value was stable over all sample measurements (during a period of 7 days). Four weeks later, during which the Autosal had not been used, the *zero* reading was 0. The stability over the measurement period is the critical factor.

Initially the Autosal heaters were observed to be permanently off. No heater cycling could be observed. On investigation the power lead to the heat extractor fan was found to be detached. It was likely that this occurred when the Autosal tank had been filled. When the salinometer is opened, and the tank slid forward to allow access for filling, the electrical power lead from the salinometer to the extractor fan mounted on the rear case of the salinometer is too short.

The salinometer was situated in the Micro-Radio Room (MRR). The air temperature in the MRR is controlled in the following way: one, the temperature of the air supplied to the air conditioning is modified by adjusting the flow of hot water through a heat exchanger; two, by adjusting a reheat thermostat controlling an electric heater situated within the air conditioning, close to the vent in the MRR. Step one has to be adjusted by the ship side Engineering Department and two allows local control within the MRR. The easiest approach to obtain reliable temperature stability is as follows. Switch off the reheat thermostat in the

MRR. Have the Engineering Department adjust the heat exchanger to supply air to the MRR at about 2 to 3 °C below that required. This step is not precise. Then use the reheat thermostat to raise the air temperature to that required. It was found that if the air flowing into the MRR (measured just downstream of the reheat element) was 1 to 2°C colder than the mean air temperature of the MRR, lights, Autosal and bodies provided the additional heat required.

In Port the Chief Engineer stabilised the MRR at 22.0 ± 0.5 °C. With the Autosal bath temperature set to 24°C. However, on crossing the Polar Front the outside air temperature dropped to -1.5°C, very close to the sea-surface temperature. The (MRR) temperature dropped by several degrees. Again the Chief Engineer was required to adjust the inlet air temperature. Adequate temperature stability could only be achieved at 19.0 ± 0.5°C. The Autosal bath temperature was then set to 21°C and left to re-equilibrate at this new temperature.

Samples from stations 02 through 14 and the first 24 underway surface salinity samples were analysed with the bath temperature set to 24°C. For the remaining samples a bath temperature of 21°C was used.

The distilled water was highly aerated water supply. When flushing the cell with distilled water many small bubbles were seen to be flushed into the measuring cell. This effect did not occur if the distilled water was left overnight before being flushed through the cell. Highly aerated distilled water is not a concern. However, it later seemed further evidence for sample degassing which was sometimes problematic and which is discussed below.

Bubbles appearing in the cell of the Autosal introduced via the inlet tube have been noted on recent past cruises in high latitude regions, [Bacon, 1993], [Bacon, 1993]. We believe that a similar effect was observed during this cruise. Highly oxygenated, cold samples equilibrating to a higher temperature have less ability to hold gas in solution. The salinity samples appear not to equilibrate (in gas concentrations) for their new equilibrium temperature before analysis. The speculation is that increased agitation through the peristaltic pump and through metal/plastic pipe junctions in the Autosal heat exchanger encourage bubbles to form as the samples out-gas. These bubbles eventually appear (sometimes as a

stream of bubbles) in the Autosal cell: leading to unstable noisy readings. This was dealt with by pumping the sample side of the Autosal clear of all sample and flushing with air. If this was done as required then the Autosal readings were satisfactory. See [*King and Alderson*, 1994] for a more detailed discussion of these effects.

384 CTD salinity samples and 65 underway salinity samples were analysed using 30 ampoules of P120 standard sea water. Of these, 2 ampoules of standard sea water were unusable because the necks were too narrow to allow the peristaltic pump tube to enter. No duplicates (samples drawn from different Niskins closed at the same depth) or replicates (two or more samples drawn from the same Niskin bottle) were drawn.

A comparison of salinity measurements was made with the results of [*King and Alderson*, 1994]: an idendical section made in 1993.

From [*King and Alderson*, 1994] it is seen that there is a linear θ/S relationship in the deep water of the Drake Passage for -0.3 < θ < 0.6, 34.66 < S < 34.71.

Linear least squares regression between bottle salinities and up cast potential temperatures are given in Table 1 for:

$$\theta = A + B \times S \tag{1}$$

Figure 1 shows the fits given in Table 1. In the deep water at a potential temperature of -0.2 °C the R94 data are fresher by about 0.002 psu, which reduces to 0 psu at 0.6 °C. The difference in the deep water cannot be accounted for by differences in standard sea water as [*King and Alderson*, 1994] used the same batch as reported here. A more detailed statistical approach should reveal whether this difference is significant.

1.1.1 Oxygen Isotope Samples

In addition to salinity samples, oxygen isotope samples were drawn at each station and depth. These were stored in small, wax sealed winchester bottles for post-cruise analysis on return to the U.K. These samples were drawn for Russell Frew, University of East Anglia.

1.2 CTD Package and Deployment

1.2.1 CTD Frame and Termination

The BAS CTD frame is adequate for CTD deployments with a 12 position GO Rosette and 1.7l bottles. The lifting arrangement is as follows: four wire strops are attached

by shackles to four points on the top of the frame. The strops are then attached by shackles to welded metal rings, one for each strop. These metal rings are in turn attached to a larger single metal ring. This larger metal ring is then in turn attached by shackle to the eye around which the CTD cable is bent. The CTD termination cable must then be lead down between this mess of strops, shackles and rings. Consequently there is chance of wear or damage to the termination. Twice during the cruise the termination came under strain causing it to fail. Once when a strop became entangled and a second time when after the four strops had been replaced due to wear on the old ones insufficient care was exercised to check that the termination length was sufficient: it was not and was pulled apart on deployment. Some simplifiction of the lifting arrangement is desirable.

1.2.2   Gantry and Winch

The CTD was deployed from the amidships gantry. All deck operations were undertaken by deck crew. On deployment and recovery light throwing lines were used to maintain close control of the package.

A 10T traction winch was used to haul the package on the 10 mm Rochester single conductor cable.

At the end of each down cast a cable washing system had to be fitted: this took five minutes. The package was hauled 50 m clear of the bottom before the cable washer was fitted, ensuring the safety of the package close to the bottom.

1.2.3   Pylon and Water Bottles

After teething problems, due to difficulties with the termination, the GO 12 position pylon worked satisfactorily. Occasional misfires were reported which in fact had fired a bottle. Only on one occasion did the pylon misbehave. This was on station 21 after a partial flooding of the termination at 4000 m caused an intermittent short to the power supply.

The deck unit in operation with the pylon did not allow uninterrupted power to the CTD during bottle fires. This created bad CTD data during firing of bottles. A switch was fitted between the deck unit and the Level A which allowed the data stream to the Level A to be interrupted at bottle firing. This procedure meant that during the bottle fire there is a time

gap of approximately 45 second in the CTD data stream. However, this time gap provided a robust marker to indicate bottle fires.

The bottle depths are shown in Figure 2. These depths were chosen to coincide with the depths sampled by [*King and Alderson*, 1994].

The following was noted about the BAS 1.7l GO sample bottles. First, bottle 1 had smashed rosette mountings. This loss was particularly unfortunate as it was one of only three bottles with reversing frames. Second, being old bottles two different types of air vent were used. One had a narrow threaded plastic bung. Two of these sheared when being closed for the first cast. A spare was taken from bottle 1 and the second was replaced by a stainless washer and bolt. Samples being obtained by allowing air to fill the bottle by tipping the top end cap.

The following bottles all had intermitant leaks at petcocks and/or O-rings: 3, 11, 5, 6, 10, 4. In addition bottles 5 and 6 had weak bungee.

1.3   CTD Operation, Data Capture and Calibration

The following instruments were fitted to the underwater package:

1. Neil Brown Mk III CTD (no oxygen sensor). *S/N 01-3838-1086* , conductivity cell *S/N C75* (BAS)

2. 12 x 1.7 litre GO rosette (BAS)

3. Three SIS digital reversing thermometers and one SIS precision reversing pressure meter (IOSDL)

4. 10 kHz pinger for near bottom approach (BAS)

The shipboard equipment consisted of:

1. Neil Brown Mk III deck unit and GO water bottle firing unit.

2. IBM PS2 system employing EG&G CTD data acquisition firmware for real time display of data and raw data backup by dumping disk files onto a tape streamer.

3. Primary data acquisition was via the shipboard Level ABC system.

1.3.1   Data Capture

CTD data were passed from the CTD Deck Unit to the Level A dedicated microcomputer. In real time this despiked the data and computed one second averages. The

time rate of change of temperature was also computed over the one second average. These averages were then passed to the Level B, a SUN workstation. These data are passed to Level C archiving. [*Pollard et al.*, 1987] gives an account of this system.

The Level A was prone to serial over-runs. The cause of this is unknown but under investigation. The result was the loss of a few seconds of data from each cast. Thus losing a few (2 to 4 dbars) of data at each over-run.

A more serious problem was when the Level A "locked" failing to pass data to the Level B, constituting a loss of data. This was inconvenient as the data had to be recovered later from the pc and processed using software written to imitate Level A operations. On one occasion after a Level A crash, on re-set the time base jumped ahead. Again the reason for this is not yet know, but under investigation.

1.3.2   Temperature Calibration

CTD temperature was calibrated at IOSDL on 24 June 1994 (Issue no. CT007) at 13 temperatures on the ITS-90 scale, at temperatures between -2°C and 25°C. The transfer standard had been calibrated at the triple points of Mercury and water, and at the melting point of Gallium.

Initial investigation of the temperature calibration had shown an unsatisfactory non-linear response near zero degrees centigrade, with errors of up to 5 millidegrees. This is associated with the electronics of the instrument near the change of sign. Accordingly, a temperature offset of about 2°C was introduced, so that likely oceanographic temperatures were all reported by the instrument as positive. The offset had the added effect of reducing the maximum operating temperature of the instrument by 2°C as well, to about 30°C.

The following calibration was applied to CTD temperature data:

$$T = -2.0887 + 0.99055 \times T_{raw} + 0.6380E - 5 \times T_{raw}^2 \tag{2}$$

This calibration was in degrees C on the ITS-90 scale, which was used for all temperature data reported from this cruise. For the purpose of computing derived oceanographic variables, temperatures were converted to the ITS-68 scale, using:

$$T68 = 1.00024 \times T90 \tag{3}$$

as suggested by [*Saunders*, 1990].

The mismatch between the time constants of the temperature and conductivity sensors is minimised using a time constant, $\tau = 0.20s$ in:

$$T = T + \tau \times \Delta T \tag{4}$$

where ΔT is the time rate of change of temperature over a one second temperature sample (32 Hz) computed in the Level A, as described in the SCOR WG 51 report [*Crease and al*, 1988].

1.3.3   Pressure Calibration

CTD pressure was calibrated at IOSDL on 27/6/94 (Issue no. CP0004) at 14 pressures between 0 and 6000 dbar, and at temperatures of 20°C, 10°C and 1°C. The calibration was performed using a dead-weight tester in series with a Paroscientific Digiquartz model 240 portable transfer standard; the Digiquartz was taken as the standard. The resulting calibration information was analysed for temperature dependence and hysteresis between calibrations at increasing and decreasing pressure.

As [*King and Alderson*, 1994] found the pressure offset varied with temperature. This effect had not been noted before as the pressure calibration had never been done at different temperatures. The mean in situ temperature of the Drake Passage Section in 1993 was 1.4301 °C with a standard deviation of 1.2265 °C: the pressure calibration at 1°C was applied:

$$P = -6.8 + 0.99917 \times P_{raw} - 2.96E - 7 \times P_{raw}^2 \tag{5}$$

followed by the temperature dependent pressure offset correction:

$$\Delta P = \left(T_{lag} - 10.0 \right) \times \left(-0.08 + 5.0E - 5 \times P + 1.4E - 9 \times P^2 \right) \tag{6}$$

Here T_{lag} is a lagged temperature, in degrees C, constructed from the CTD temperatures. The time constant for the lagged temperature was 400 seconds. Lagged temperature is updated in the following manner. If T is the CTD temperature, t_{del} the time interval in seconds over which T_{lag} is being updated, and t_{const} the time constant, then:

$$W = \exp\left(-t_{del} / t_{const} \right) \tag{7}$$

$$T_{lag}\left(t = t_0 + t_{del} \right) = W \times T_{lag}\left(t = t_0 \right) + \left(1 - W \right) \times T\left(t = t_0 + t_{del} \right) \tag{8}$$

The value of 400 seconds for t_{const} is based on laboratory tests.

A final adjustment to pressure is to make a correction to up cast pressures for hysteresis in the sensor. This is calculated on the basis of laboratory measurements of the

hysteresis. The hysteresis after a cast to 5500 m (denoted by $dp5500(p)$) is given in Table 2. Intermediate values are found by linear interpolation. If the observed pressure lies outside the range defined by the table, $dp5500(p)$ is set to zero. For a cast in which the maximum pressure reached is p_{max}, the correction applied to the up cast CTD pressure (p_{in}) is:

$$P_{out} = p_{in} - \left(dp5500(p_{in}) - \left((p_{in}/p_{max}) \times dp5500(p_{max})\right)\right) \tag{9}$$

1.3.4   Conductivity Calibration

The conductivity sensor was calibrated on 04/06/94, (Issue no. 90924), by calibration against a Guildline Autosal Model 8400B, S/N 238707 standardised with standard sea water batch P123. The following calibration was obtained:

$$C_{new} = 0.00955 + 0.9783 \times C_{old} \tag{10}$$

This was followed by the cell material deformation correction:

$$C_{new} = C_{old} \times \left[1 + \alpha \times (T - T_0) + \beta \times (P - P_0)\right] \tag{11a}$$

where the coefficients for the cell material are:

$$\alpha = -6.5E^{-6}{}^{\circ}C^{-1} \tag{11b}$$

$$\beta = 1.5E^{-8}dbar^{-1} \tag{11c}$$

$$T_0 = 15^{\circ}C \tag{11d}$$

$$P_0 = 0dbar \tag{11e}$$

and P, T and C_{old} are CTD pressure, temperature and conductivity.

The conductivity cell was found to be defective: revealed by a severe hysteresis between down cast and up cast conductivities, and by large station to station changes in the conductivity offset and slope corrections. The cell $C75$ was an old cell which had been returned to the manufacturers for re-platinisation of the electrodes.

Typically, over a range of 0 to 100 mmho/cm the accuracy of the cell should be about 0.0015 mmho/cm with a resolution of 0.000002 mmho/cm. More importantly, conductivity electrodes drift at varying rates, 0.01 mmho/month may be typical. This requires that the calibration is constantly updated. It is, in practice, preferable to group stations for determining a conductivity calibration. The assumption is that the CTD sensor is stable and that by fitting over a group of stations the uncertainty of water sample variability is reduced.

We found for the cell C75: one, hysteresis between down and up casts, amounting to up to 0.06 psu at the surface; two, a large station to station offset in salinity (and hence conductivity), of order 0.05 psu per station. The method by which the second problem may be dealt with is by determining a conductivity calibration on a station by station basis, admitting that an increase in uncertainty in the calibration will result. However, before that can be done the hysteresis in conductivity must be eliminated. The excellent report by [Millard Jr. and Yang, 1993] documents the theory and practice of CTD conductivity calibration.

To determine the relationship between the down and up cast conductivities they were matched on pressure. Conductivity, salinity and in situ temperature differences were then computed at each level. The difference data were then further selected by keeping differences only where the in situ temperature difference was within $0 \pm 0.001°C$. For shallow stations with more natural variability between down and up cast this was relaxed to $0 \pm 0.003°C$. In the deep water, were the natural variability is least and the water most homogeneous, a pressure match between down and up will reasonably match water parcels. In situ temperature is probably a better water parcel marker than pressure, however matching introduced prohibitive additional computation that was not considered to be useful.

On plotting (down-up) cast conductivity differences a linear relationship with pressure was found for all stations. It is not understood whether this represents a real pressure effect on a failing conductivity cell or whether pressure fortuitously provides a useful variable for describing a model of the (down-up) cast conductivity differences. Note that in practice a model was constructed for the *salinity* differences rather than the *conductivity* differences. Once the old up cast salinity had been corrected a new up cast conductivity was calculated.

The following up cast salinity correction ΔS_{up} was computed:

$$\Delta S_{up} = \left(S_{down} - S_{up}\right) = A + B \times P \tag{12}$$

where new up cast salinity is:

$$S(new)_{up} = S(old)_{up} + \Delta S_{up} \tag{13}$$

The new up cast conductivity is then obtained from:

$$C(new)_{up} = SAL78\left(S(new)_{up}, T, P\right) \qquad (14)$$

where $SAL78$ is the equation of state converting salinities to conductivities. Table 3 contains model coefficients for (12).

The coefficients $A1$ and $B1$, Table 3, are a second set of up cast salinity correction parameters, obtained after the first conductivity calibration and applied before the final salinity calibration discussed elsewhere. Figures 3a to 3d show the coefficients A and B, the salinity correction at the maximum pressure of the station $A + B \times P_{max}$ and R^2. The salinity correction at the minimum pressure is just $A + B \times P_{min}$ with $P_{min} = 0$ and hence is equal to the coefficient A. Stations 23 and 18 appear anomalous. No particular reason was found for this. Stations 32 and 33 are shallow.

Figures 4a and 4b show the bottle - up cast conductivites after the conductivity up cast correction and before the station by station conductivity calibration, plotted against station number and against pressure. Note the large station to station changes in conductivity of the order 0.025 mmho/cm and over the cruise of order 0.15 mmho/cm (~1.0 mmho/cm/month). This is to be compared with a typical sensor drifts of the order 0.01 mmho/month. Thus the drift in the sensor is two orders of magnitude worse than can be reasonably expected ! Because of the large scatter no apparent depth dependence of residuals is evident in Figure 4b.

Having corrected the up cast conductivities we then determined a station by station conductivity calibration. Bottle conductivities were regressed against (bottle - up cast) conductivities to obtain coefficients for the conductivity sensor model (10). Bad data were eliminated by eye where the data seemed "obviously" bad.

Figures 5a and 5b show the station by station trends for the conductivity offset and slope calibration coefficients.

The conductivity calibrations in Table 4 were applied followed by the material deformation correction (11a). We then recomputed a new correction for the upcast conductivities as described earlier, coefficients $A1$ and $B1$ in Table 3. Figure 6a and 6b shows the (bottle - up cast) conductivity differences plotted against station number and against pressure. These figures may be compared to Figures 4a and 4b. The station by station

trends in conductivity difference have now been reduced. A noticeable depth dependence remains. This could be due to some other physical effect of the instrument or could be a description of the lack of fit of the model used to correct the up cast conductivities. In the second case nothing could be done except to fit a more sophisticated model to correct up cast conductivities. In the first case however an appropriate salinity correction could be applied.

The mean (bottle - up cast) conductivity difference is 0.0001 mmho/cm with a standard deviation of 0.0034 mmho/cm for 251 out of 289 samples. The scatter is about twice what one might expect for a good cell.

1.3.5 Salinity Calibration

Having observed a systematic depth dependence in the bottle - up cast conductivities and in the (bottle - up cast) salinity differences a final salinity calibration on a station by station basis was made by fitting the residuals with:

$$dsalin = a + b \times P + c \times T \tag{15}$$

The most likely reason why this fit was necessary is that the conductivity offset and slope corrections were not determined with sufficient accuracy with a maximum of 11 bottles per cast over the water depth. Errors in these model coefficients would lead to a systematic depth dependence in salinity through the effects of the *non-linear* equation of state for sea water.

The *dsalin* correction at (P_{max}, $T(P_{max})$) may, in normal circumstances, be used as an estimate of the cell drift. However, here we should have accounted for the cell drift and *dsalin* thus represents the remaining (random) errors left from the original fit (which will of course be removed by the correction).

The corrections at P_{max} and P_{min}P can be seen in Figures 7a and 7b and are tabulated in Table 5 with the coefficants for (15).

1.3.6 Reversing Pressure and Temperature Measurements

Four reversing instruments were available: three SIS RTM's and one SIS RPM.

1.3.6.1 Reversing Pressure Measurements

One digital RPM was available:

Rosette position   Pressure Meter

1   P6132H

P6132H was calibrated by the manufacturer on 22/02/90 and the following calibration data were supplied:

(P6132H pressure (dbars), correction applied (dbars)), (6,-6), (975,+12), (1949,+12), (2930,+12), (3919,+8), (4907,-4), (5405,-11), (6022,-22).

The last point is an extrapolation.

The following equation was used to correct the RPM data:

$$P = -6.0 + 1.01493 \times P - 2.941E - 6 \times P^2 \qquad (16)$$

and fits the manufacturers calibration data to better than 1 dbar.

The (P6132H - up cast) pressure differences against depth. are 0 dbars at 0 dbars, up to -18 dbars at 3500 dbars and -12 dbars at 4500 dbars. This is typical of residuals observed with this RPM, as observed on WOCE cruise A11 in 1993, [Saunders, 1993] when using an IOSDL CTD.

For comparisons deeper than 1500 dbars the mean pressure difference is -14.4 dbars with a standard deviation of 2.2 dbars (22/32 points). For the A11 cruise a mean difference over the same depth range was 14 dbars.

1.3.6.2 Reversing Temperature Measurements

The digital RTM's were calibrated using the linear fits given in Table 6.

$$T_{cal} = A + B \times T_{raw} \qquad (17)$$

Table 7 gives the means and standard deviations of the temperature residuals (RTM - CTD).

The mean (RTM - CTD) temperature difference is 4 millidegrees with a standard deviation of 1.6 millidegrees. [King and Alderson, 1994] noted the the BAS CTD changed its temperature calibration by 3.5 millidegrees between calibrations. However, until we have further evidence from the next CTD temperature calibration the CTD temperature data are concluded to be satisfactory.

1.3.7   Peroration on the salinity data

Figure 8a) and 8b) summarise the final (bottle - upcast) salinity differences. The mean difference within $0 \pm 0.01 psu$ is −0.0001 with a standard deviation of 0.0018 .for 251 out of 281 samples. What must remain in mind is this: due to a failing conductivity cell a model of

the difference between down and upcast conductivities has been constructed. The object of this model was to correct the observed hysteresis between down and up casts. This correction to upcast conductivities then allowed a typical calibration to be done against salinity samples. This process was necessary because it was impossible to achieve a satisfactory match between down cast data and bottles in the variable upper layers. The extent to which we believe the residulas described above represent the real CTD data errors is entierly dependant on our simple linear correction of the upcast conductivities.

1.4   Underway Observations

1.4.1   Thermosalinograph

To calibrate the thermosalinograph (TSG) salinity samples were drawn from the TSG tank overflow at two hourly intervals.

A SEA-BIRD ELECTRONICS thermosalinograph was run continuously where ice conditions allowed. Samples for calibration were drawn only on the southward crossing of the Drake Passage. The TSG was calibrated on 21/06/94. The temperature sensor (no. 593) gave a mean difference to a bath temperature of 0.00017 °C with a standard deviation of 0.00084 °C. The temperature sensor (no. 820) gave a mean difference to a bath temperature of 0.00011 °C with a standard deviation of 0.0009 °C. The conductivity sensor (no. 820) gave a mean difference to a salt bath of -1.0E-05 mmho/cm with a standard deviation of 5.3E-04 mmho/cm. Note that the surface temperature sensor was digitised to 0.1 °C.

TSG salinity measurements at 10 second intervals were averaged to 2 minute intervals and then median despiked, discarding data more than 0.01 psu from a mean computed over 5 adjacent data values. The data were further despiked by hand and then filtered using a top hat filter (sum of weights = 1) with a width of 30 minutes. These data were then merged with the underway salinity samples and the underway salinity minus TSG salinity difference computed. This difference was filtered with a top hat filter (sum of weights = 1) with a width of 28 hours and was then added to the TSG salinities.

The mean difference (within $\pm 2\sigma$) for the TSG minus bottle salinities is 0.0012 psu with a standard deviation of 0.0193 for 54/57 samples.

Figure 9 shows TSG surface salinity and temperature and surface salinity samples.

1.4.2 Echosounding

The *James Clark Ross* is fitted with an IOS Mk IV PES, whose display is located in the UIC lab, and a Simrad EA 500, whose display and controls are located in the wheelhouse. The EA 500 depths were logged via a level A as usual. The EA 500 data were also logged to colour hardcopy in the wheelhouse. It was realised near the end of the cruise that the sound speed assumed in the EA 500 software was 1471m/s and not 1500m/s as required by Matthew's or Carter Table corrections. In order to apply the RVS prodep correction to the data, depths in the raw data files were first scaled by 1500/1471.

The PES display in the UIC lab was also used for monitoring the 10 kHz pinger on the CTD rosette during near-bottom approaches.

1.5 XBTs

Eleven XBTs (T7s) were deployed from a hand-held launcher attached to a Sippican Mk 9 deck unit interfaced to a PC. Table 8 gives station positions. The data were logged using the Sippican software on the PC into files with extension SIP, and then converted into files with depth/ temperature pairs with extension EXP. These ASCII files were transferred for further processing on the SUN sytem using floppy disks.

These data were then converted into PSTAR format. A program written at the James Rennell Centre by Mike Griffiths was then used to convert the profiles into TESAC message format. This is a general purpose routine which also works with CTD and ADCP data.

One problem encountered with the XBT system concerned the electrical connection between the XBT probe and the launcher. It was discovered that on attempting to enter the launch mode on the PC, the software would not recognize that a probe had been loaded. This could be resolved by removing and reloading the probe repeatedly until the software responded.

1.6 Acoustic Doppler Current Profiler (ADCP) Measurements

1.6.1 Instrument performance

The *James Clark Ross* has a 150 kHz RDI unit, hull-mounted. The transducer is offset from the fore-aft direction by approximately 45 degrees. On this cruise the firmware version was 17.07 and the data acquisition software (DAS) was 2.48. For the transects across Drake

Passage, the instrument was used in the water tracking mode, recording 2 minute averaged data in 64 x 8m bins. 'Blank beyond transmit' was 4m and the depth of the transducer is approximately 5 metres. On the shelf at the start of the cruise, across Burdwood Bank and after the transect for the rest of the passage, bottom tracking was used. The bottom tracking configuration had the same number and size of bins, and one bottom ping per four water pings.

In order to provide protection from ice the transducer on the *James Clark Ross* is located in a sea chest, recessed in the hull. The sea chest is closed by a 33 millimetre thick window of Low Density PolyEthylene (LDPE), and filled with a silicone oil. The temperature of the oil is measured, and returned to the DAS as "water temperature".

Depth penetration depended, as ever, on sea state. However, it can be said that reasonable data were generally collected over the upper 200-300 metres, with bottom tracking generally available in depths down to 450 metres.

Two corrections are required to the velocity data. The first concerns its amplitude which is in error mainly due to assumptions in the software about sound speed. The second concerns the alignment of the transducers with respect to the fore-aft line of the ship. Any small angular errors here transform some of the velocity of the ship when underway into calculated water velocities when the ships velocity is subtracted from the ADCP velocities. In order to determine these errors, comparisons were made between the speed and direction of the ship over the ground determined from the GPS position fixes (DGPS fixes will be used when the data are post-processed ashore), and the speed and direction of the ship over the ground from the ADCP bottom tracking. The differences should be the required corrections.

1.6.2   Determination of speed correction factor

As described in ([*King and Alderson*, 1994], the presence of the oil filled sea chest around the transducers requires a correction to all speed data computed by the RDI DAS. This is because the software computes water velocities relative to the ship using the known angle of the transducers (30° to the vertical) and the speed of sound at the transducer. If, as in this case, the fluid surrounding the transducer is oil and not seawater, the speed of sound required is that in oil. The software allows the user to specify the speed to be a fixed value

or, optionally, computed in the DAS from a fixed salinity and the temperature measured at the transducer. On this cruise the reported 'water temperature' was combined with a salinity of 35 to give sound speed. Thus a correction based on this temperature needs to be applied, specifically:

$$F = 1.0055 \times \left(1 - 0.004785 \times T + 0.0000355 \times T^2\right) \qquad (18)$$

This provides a correction factor for sound speed in seawater (at S = 35) to sound speed in the oil.

1.6.3   Determination of heading misalignment

All data were corrected for the variation in the ship's gyrocompass heading errors by employing data from the Ashtech GPS 3DF heading system, described below. Ashtech-gyro differences had been determined by comparing the two instantaneous measurements of heading, and smoothed to two minute averages. These differences were merged onto the ADCP two-minute ensembles, and relative direction modified by the addition of Ashtech-gyro difference. In principle the ADCP data were now referenced to heading determined from the GPS system, and needed to be corrected only for the fixed misalignment between the direction defined by the GPS antennas and the direction of the ADCP transducer.

The misalignment error (and any remaining amplitude error) was calculated as follows:

a)   Two-minute ensembles were merged with GPS positions which had been filtered over 2 minutes, and ship's east and north velocity calculated. Absolute ADCP bottom tracking velocity was also calculated.

b)   All good data were then listed and divided by eye into periods of between 20 and 30 minutes in which: (i) at least 10 consecutive two-minute ensembles had bottom tracking data; (ii) two-minute averages of speed had a range of no more than 20 cm/s; (iii) two-minute averages of direction over the ground had a range of no more than 20 degrees. 30 such intervals were found and then averaged together to give estimates of speed and direction from GPS and ADCP. Each average thus represented a period when the ship was steaming on a steady heading at a steady speed.

c)   The speed and misalignment errors were computed for each averaging period as (speedGPS/speedADCP) and (directionGPS - direction ADCP). The resulting direction

difference would need to be added to all ADCP directions to produce correct ship-over-ground or ship-over-water velocities.

The ratio of GPS and ADCP speeds average to 1.00 with standard deviation 0.04 units. The GPS minus ADCP directions have mean value -2.14 degrees, with standard deviation 0.30. These are remarkable results. These numbers are the same as those calculated for the previous years data [*King and Alderson*, 1994] but using differential GPS data.

1.7 Navigation

1.7.1 GPS-Trimble

Navigation during the cruise was provided by the ship's Trimble 4000 receiver, with fixes roughly once per second. Data were logged while the ship was tied up at FIPASS and at Rothera in order to assess the noise level of the positional information. RMS errors in position were calculated from the FIPASS data over 10 minute intervals. The resulting rms's have average 24m and standard error 1m. Using 20 minute intervals does not appreciatively improve the errors, so 10 minute averages have been adopted for the adcp data on this cruise. These rms errors may introduce nominal uncertainties in velocity of 4 cm/s on station. The precision should be greatly improved once differential GPS data is used.

1.7.2 Differential GPS

After the success of last year's use of differential GPS data [*King and Alderson*, 1994], the Trimble receiver on the *James Clark Ross* was upgraded in order to deliver one half of the differential signal required. The second part is to be acquired from a ground station in Santiago, Chile. It remains to be seen how successful this will be given the increasing distance between the two differential sites with time.

Raw pseudorange data were output via a serial port and the ships patch panels to a PC in one of the laboratories. Software on the PC supplied by Trimble recorded the data in sets of files on the hard disk. Data were recorded at 1 Hz in files of length 1 hour during the transect, but then the frequency was reduced to 0.1 Hz thereafter. The elevation mask for the data was inadvertently left at a default value of 15°, which will reduce the amount of useful data. A value of 5° would have been more useful.

One difficulty encountered was that the PC was not connected to the ethernet, consequently backing up the data required transfer by floppy disk, which proved onerous at times. A limitation of the PC software was that filenames were generated using a day number and a sequence number incremented from the last file present in the current directory. This meant that restarting the logging in other directories for neatness risked the creation of files with identical names on the system.

The receiver and PC ran without problems throughout the cruise.

1.7.3   Gyrocompass

The ship is fitted with two identical gyrocompasses - Sperry Mk 37. The instrument used for ship navigation was also the one logged via a level A and to provide headings to the repeaters in the labs and to the ADCP. While the ADCP is supplied via a synchro pickup, the lab repeaters measure relative changes, and have to be initialised to the correct heading individually. The ADCP and the level A receive the same voltages from the synchro pickup on the gyro, but digitise them separately. The gyrocompass in use was swapped at Rothera by the Second Officer. No problems with the gyrocompass itself were noted.

However, at the beginning of the cruise the level A was observed to only output integral values of heading. This was because of the limited resolution programmed into the level A application. The problem was resolved by swapping the gyro application EPROMS with those from an old level A.

1.7.4   Ashtech GPS3DF

An Ashtech GPS 3DF system was purchased from UK WOCE Capital funds and installed on RRS *James Clark Ross* while the ship was at Grimsby by RVS. The antennas and cables were still in place from the year before.

The receiver is located in the wheelhouse, next to the Trimble receiver. The receiver sends ASCII messages which are logged to the ship's computer system via a level A. The ASCII message $GPPAT contains time, position and attitude (pitch, roll, heading). The message is further time-stamped with ship master clock time at the level A. This ensures that the same time base is used for merging with gyrocompass data and determining gyro errors.

The antenna geometry was surveyed using the Ashtech software and data collected in Grimsby both in 1993 and 1994, but of course with different receivers. No significant differences in calibration were found. The port side aft antenna is designated as number 1; port-fwd is 2, stbd-fwd is 3, stbd-aft is 4. The relative positions are given in the table of receiver parameters below. The XYZ vectors have been adjusted so that the heading is defined by the direction normal to the 1-4 baseline, ie that baseline has Y=0.

The parameters used for this cruise were as follows (mainly set in menu 4 or its submenus).

Menu 4

```
posn            0,0,0
Alt known       N
Ranger          0
UnhealthySV     Y
Rec intvl       001
Min SV          4
elev mask       10
pdop mask       40
PortA        nmea   off
             real time      off
             VTS    off
             baud   9600
PortB (level A logging)      nmea   on
             baud   9600
             options        PAT ON
                    1 second send rate
```

ATTD CNTRL MENU

	tau	T0	Q	R
max rms	010			
search ratio	0.5			
one sec update	Y			
3SV search	N			
Hdg	999	000	1.0e-2	1.0e0
pitch	020	000	4.0e-2	1.0e0
roll	020	000	4.0e-2	1.0e0
Kalman filter reset	N			

ATTD SETUP MENU

	X	Y	Z
1-2	2.943	4.745	0
1-3	11.493	4.753	-0.006
1-4	13.222	0	0
OFFST	0	0	0
max cycle		0.200	smoothing N
max magnitude		0.080	max angle 020

Attitude data were logged at a rate of 1Hz. Following previous data processing paths, these were subjected to various data quality control procedures and merged with gyro measurements. Ashtech minus gyro headings were averaged into two minute intervals on a daily basis, of which between 80 and 95 percent contained data. Linear interpolation was employed to provide a complete set of gyro corrections. These have been used in processing the ADCP data.

The main problem encountered with this instrument was that while the ship was at FIPASS, the attitude data was poor, and based on old information. The manual suggested that low signal to noise ratios on the reception from each satellite were responsible. However the data did not improve on sailing from Stanley. Eventually, clearing external and internal memory kicked the receiver into giving sensible attitude data. The problem seemed to recur after Faraday and a second reset was performed during the visit to Rothera. The result of this second reset was not as clear cut as the first, since intermittently thereafter poor data would be recorded as the satellite configurations changed.

References

Bacon, S. (1993) A note on salts during WOCE cruise A11. *pers. comm.*

Crease, J., and e. al, The acquisition, calibration and analysis of CTD data, *Unesco Technical Papers in Marine Science, 54*, 96pp, 1988.

King, B. A., and S. G. Alderson, RRS James Clark Ross 20 Nov 1993 - 18 Dec 1993: WOCE SR1 in Drake Passage, ***, IOSDL, 1994.

Millard Jr., R. C., and K. Yang, CTD calibration and processing methods used at Woods Hole Oceanographic Insitution, *WHOI-93-44*, WHOI, 1993.

Pollard, R. T., J. F. Read, and J. Smithers, CTD sections across the southwest Indian Ocean and Antarctic Circumpolar Current in southern summer 1986/7., *Report 243*, 161 pp., Institute of Oceanographic Sciences Deacon Laboratory, 1987.

Saunders, P. M. (1990) The International Temperature Scale 1990

Saunders, P. M., RRS Discovery Cruise 199 22 Dec 1992 - 01 Feb 1993. WOCE A11 in the South Atlantic, *234*, IOSDL, 1993.

Figures

Figure 1: Potential temperature v's bottle salinities for: a) R93; b) R94.

Figure 2: Station number v's pressure showing the sampling density across the section

Figure 3: up cast salinity correction for (12); a) coefficiant A; b) coefficient B; c) salinity correction at P_{max}; d) R^2. Plotted against station number.

Figure 4: (bottle -up cast) conductivity differences after applyin equations (12) - (14) against: a) station number; b) pressure

Figure 5: Conductivity offset and slope coefficients plotted against station number: a) offset; b) slope

Figure 6: (bottle - up cast) conductivity differences after upcast conductivity correction and station by station conductivity calibration against: a) station number; b) pressure

Figure 7: SIS pressure meter (P6132H - CTD up cast) pressure against CTD pressure

Figure 8: Final (bottle - up cast) salinity differences plotted against: a) station number; b) pressure

Figure 9: TSG surface salinity, temperature and surface salinity samples

Figure 1

Bottle Depths

Figure 2

Bcoeff2.plt

Page 1

Figure 3b

Figure 3c

RSQ2.plt

Page 1
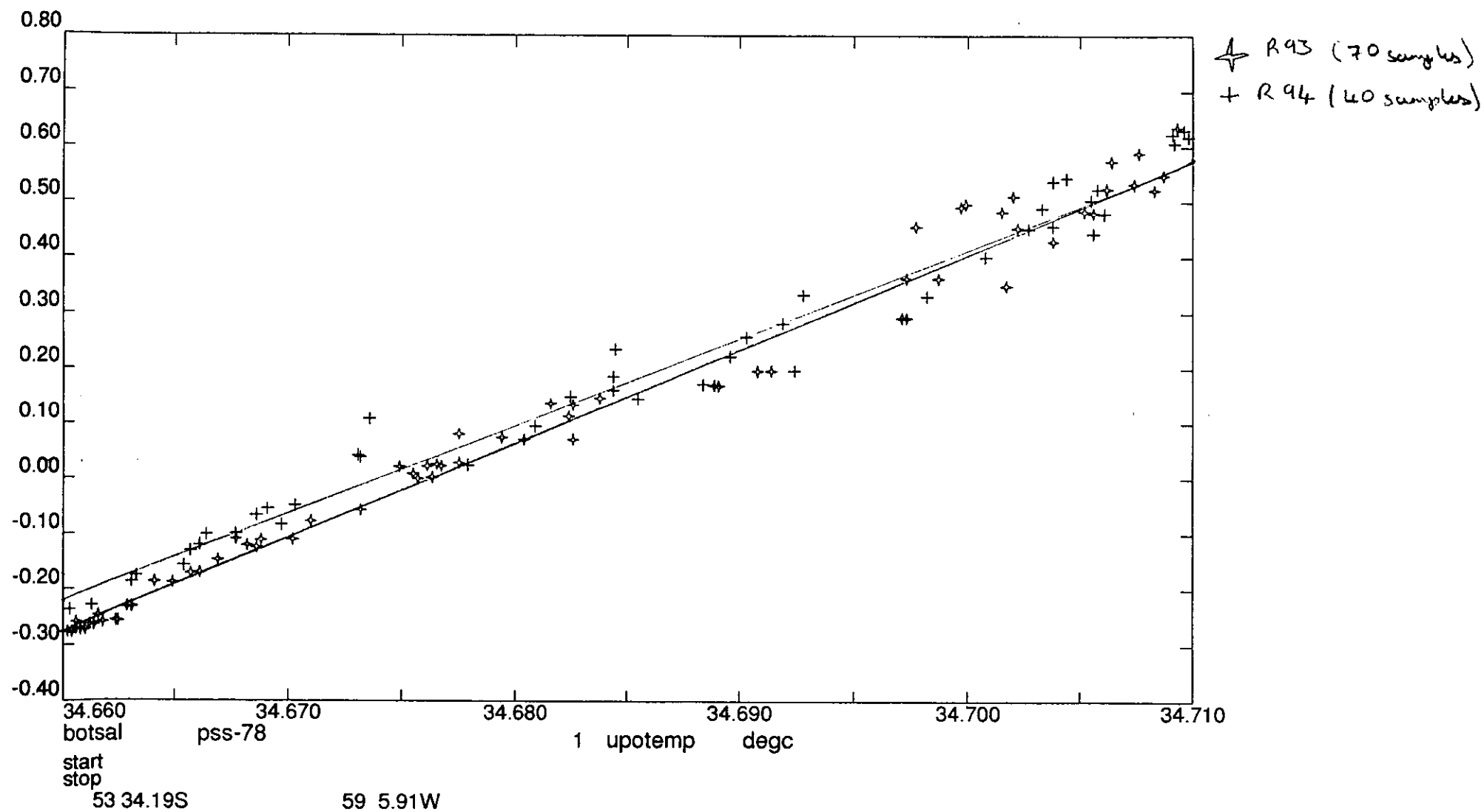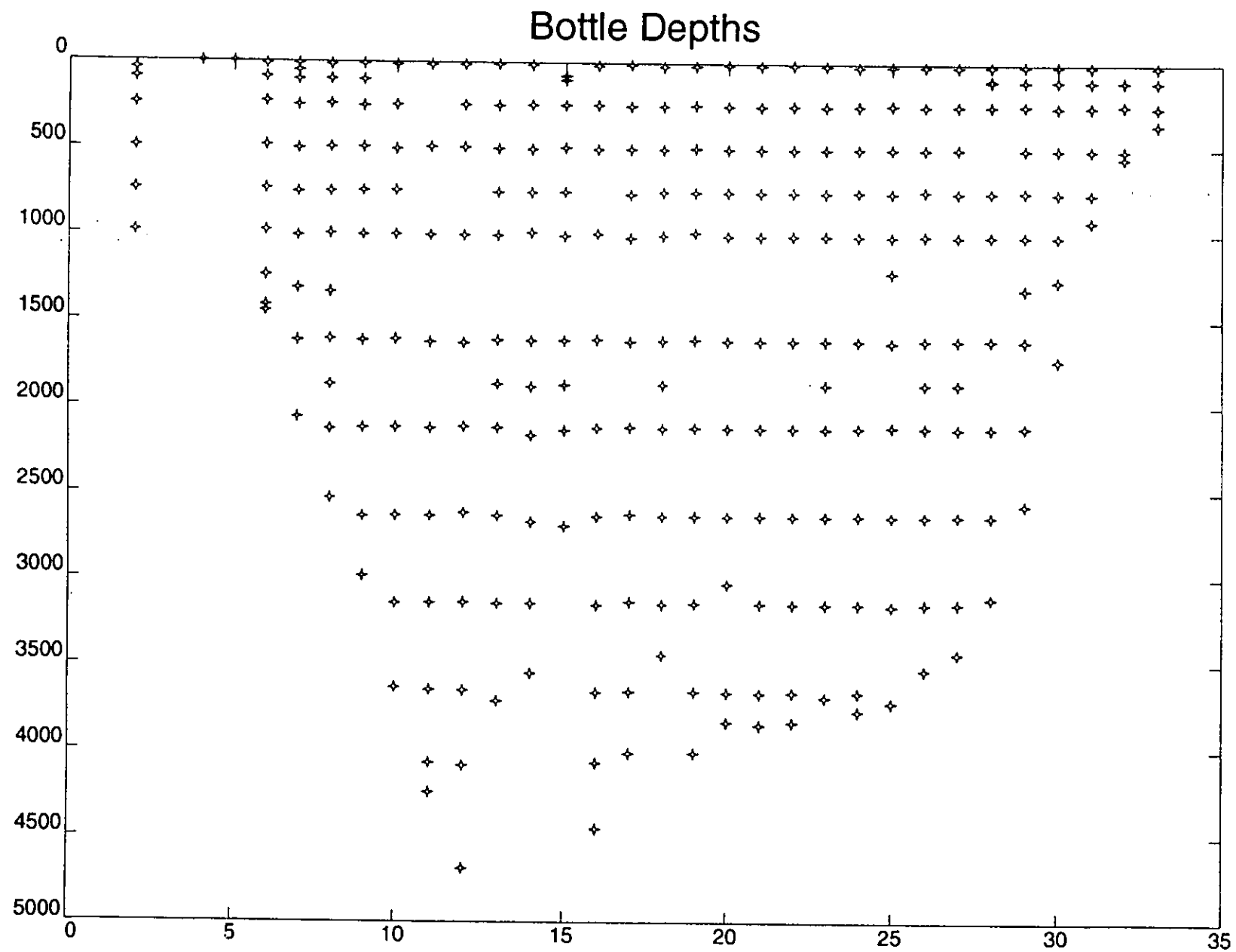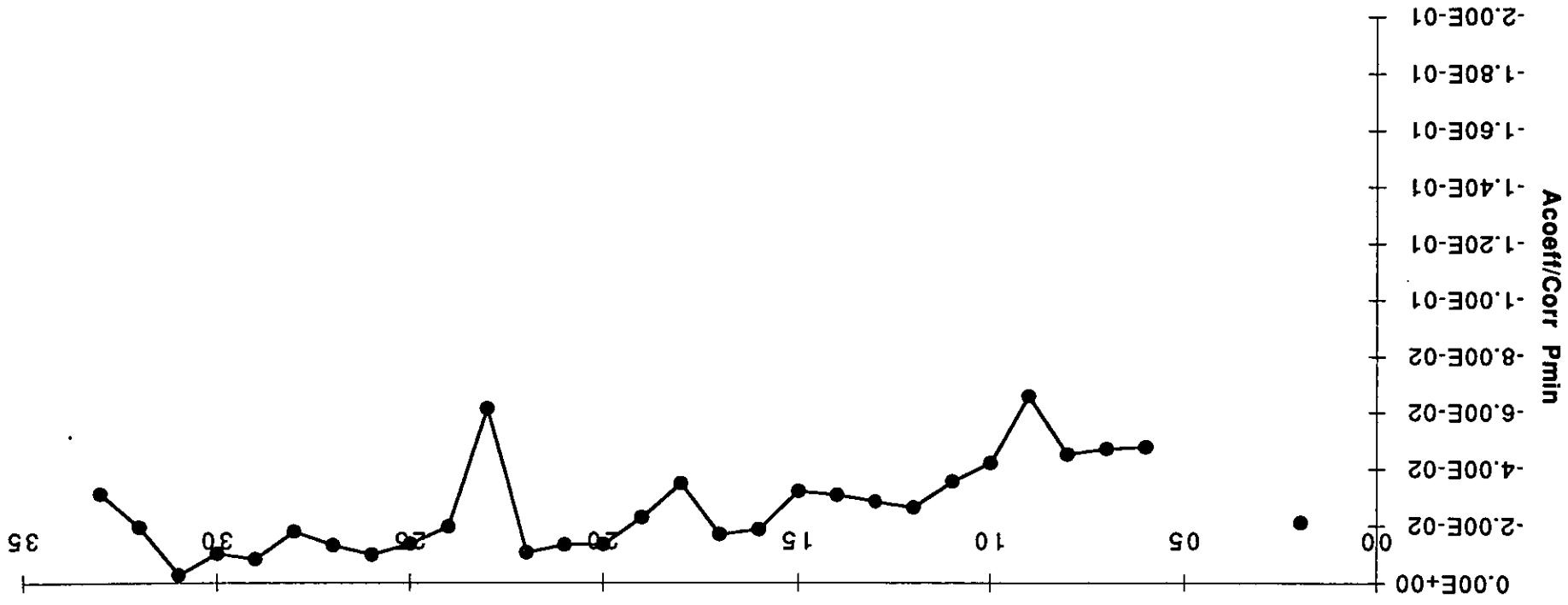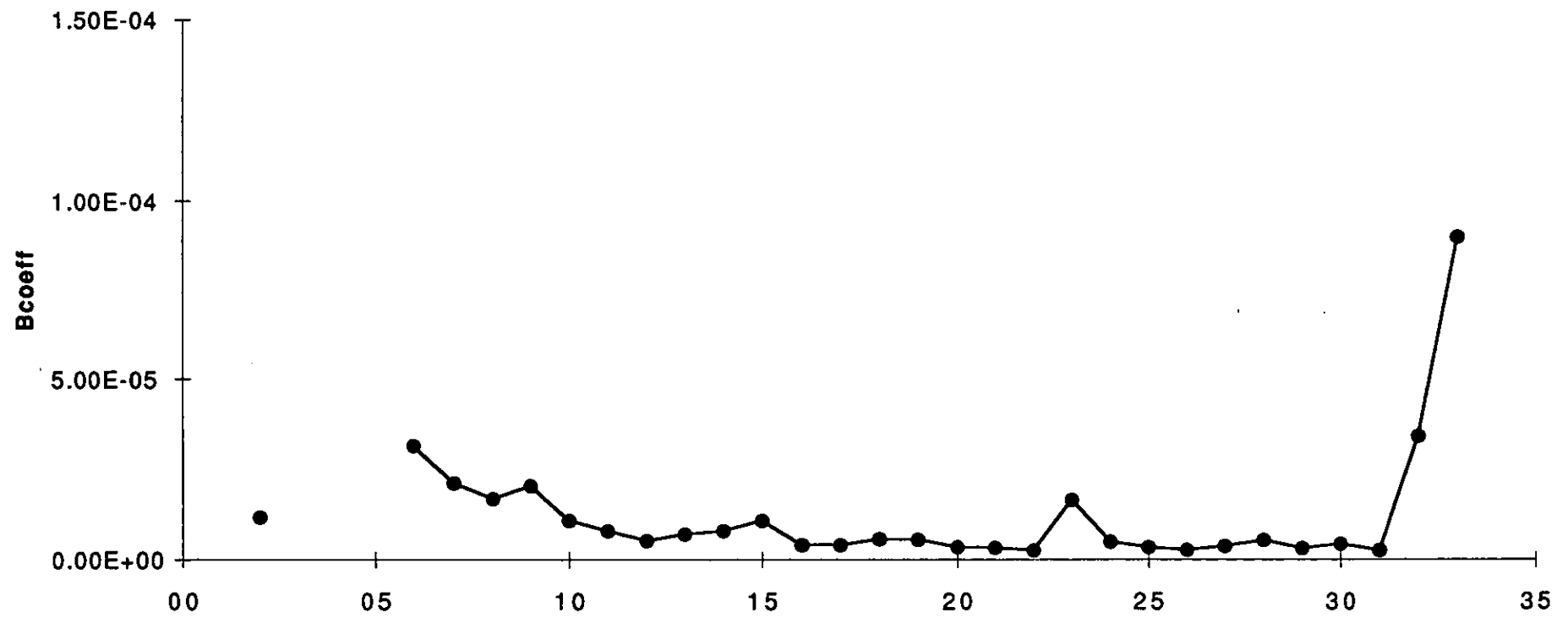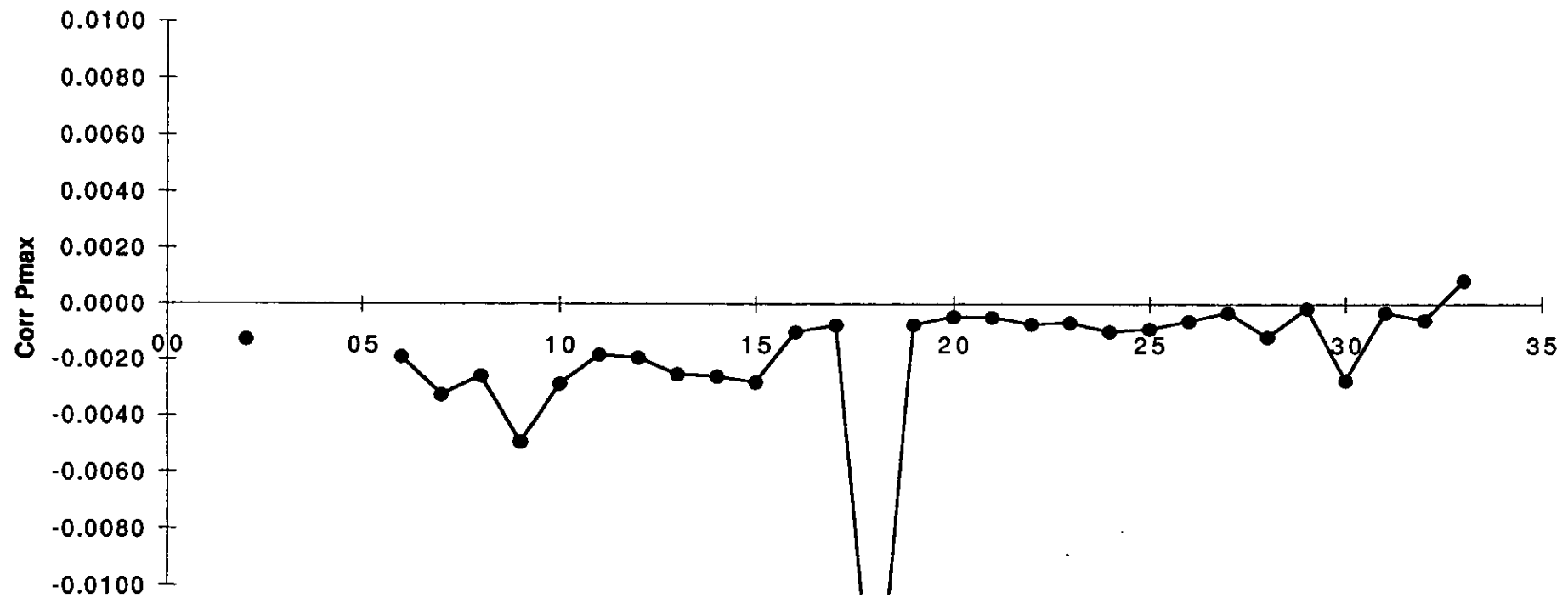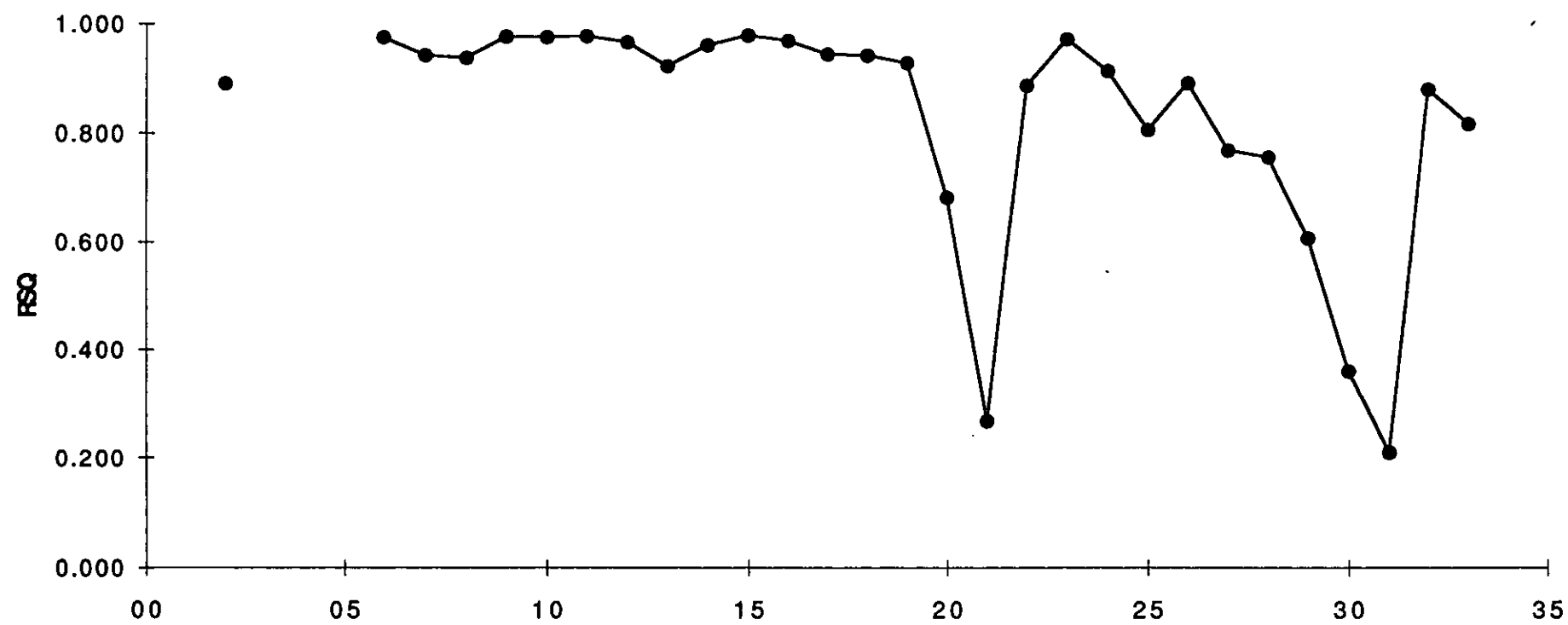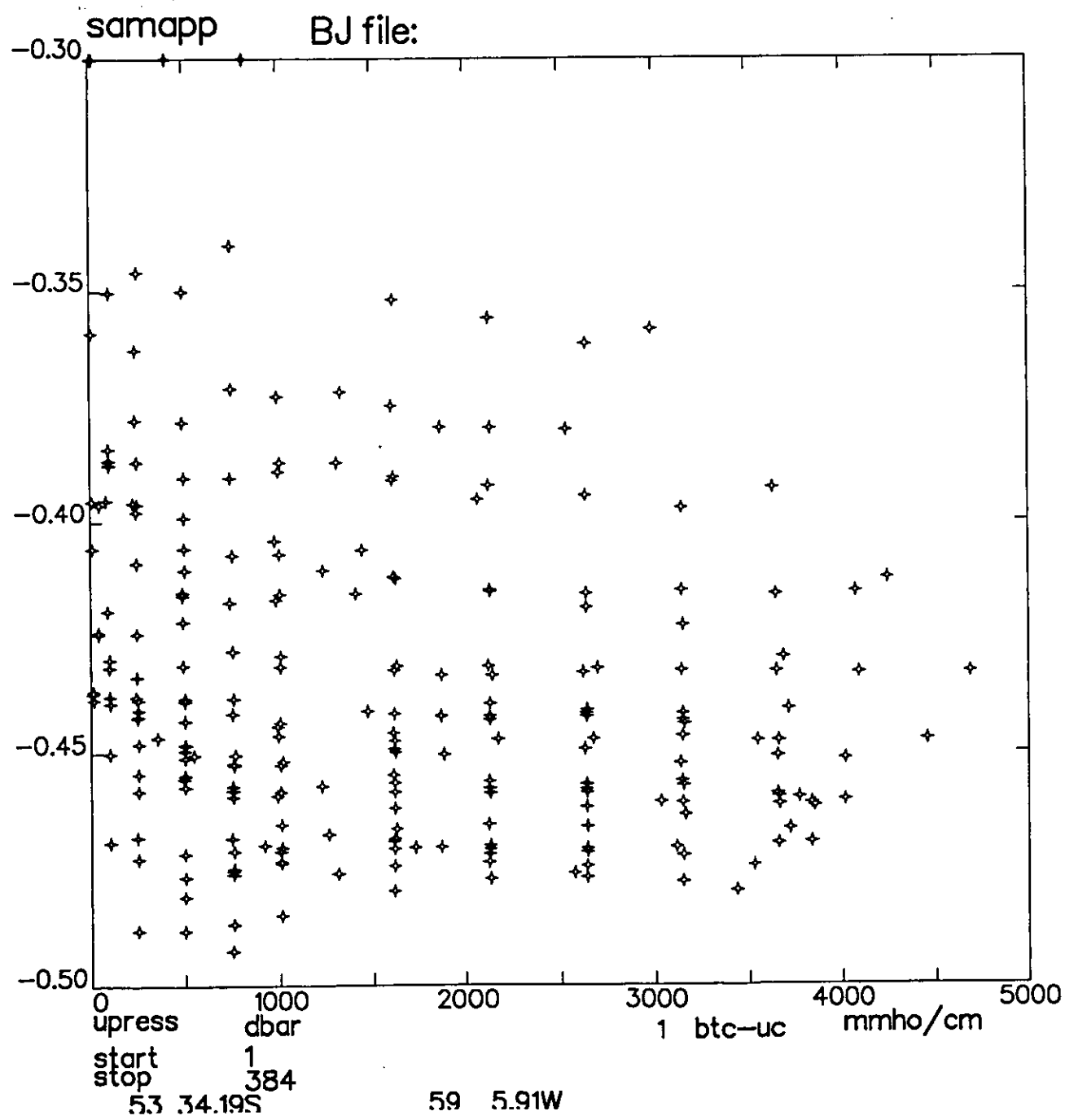
Figure 3d

Figure 4 a)

Figure 4b

cond_offset5.plt

offset

Page 1

Figure 5 a)

cond_slope5.plt

slope

Page 1
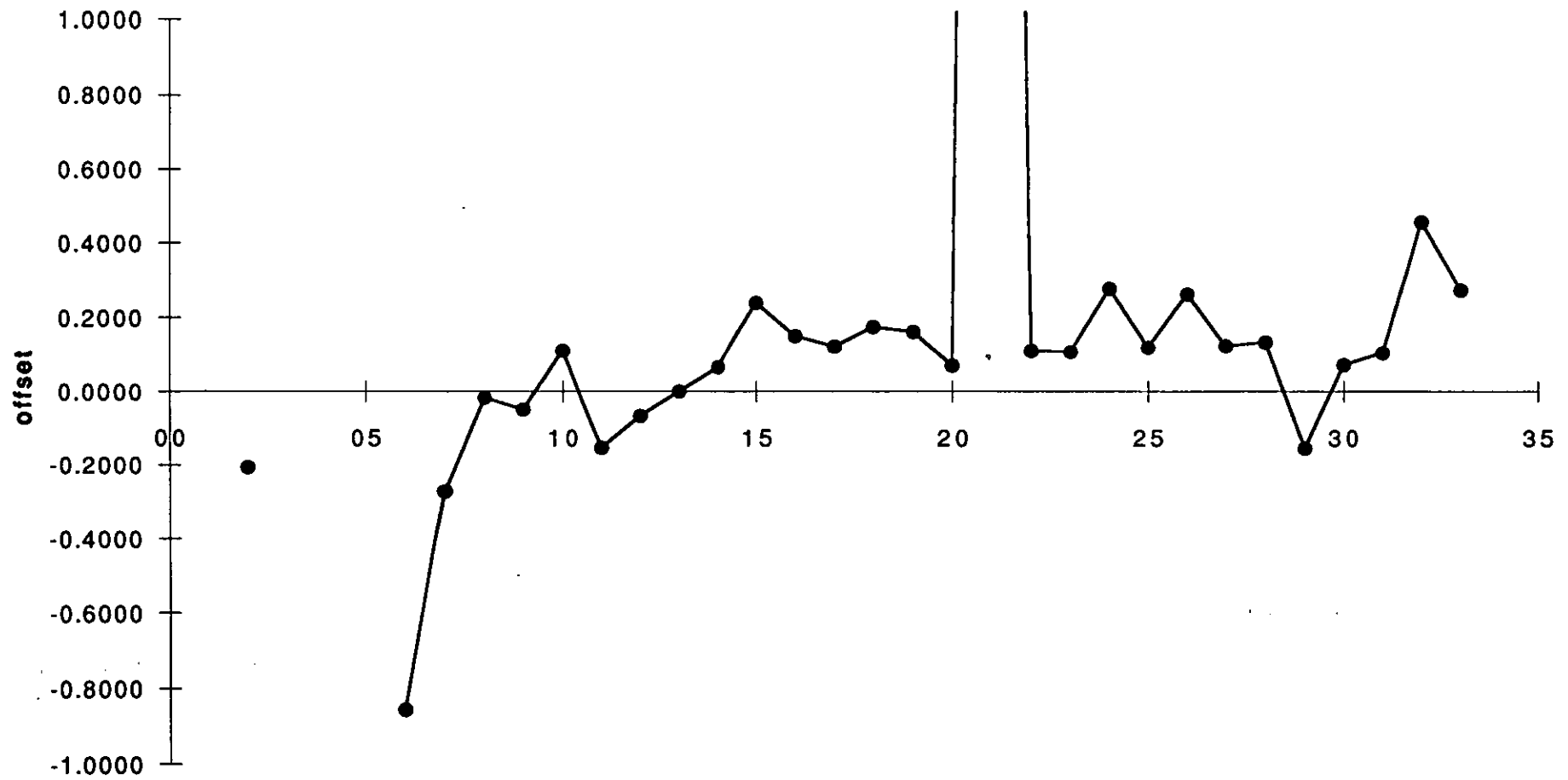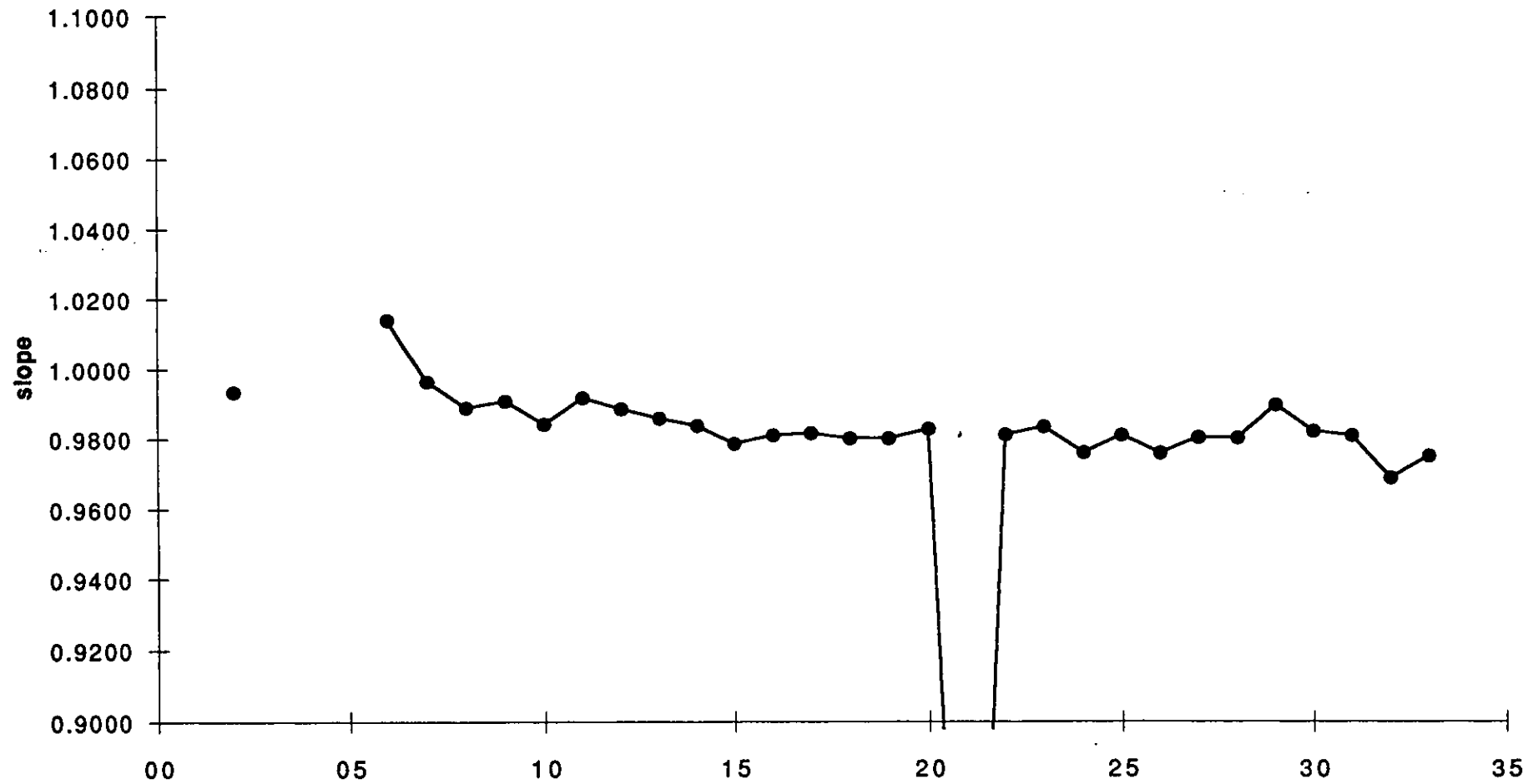
Figure 5 b)

Figure 6a)

Figure 6b)

dsalin at Pmin

station number
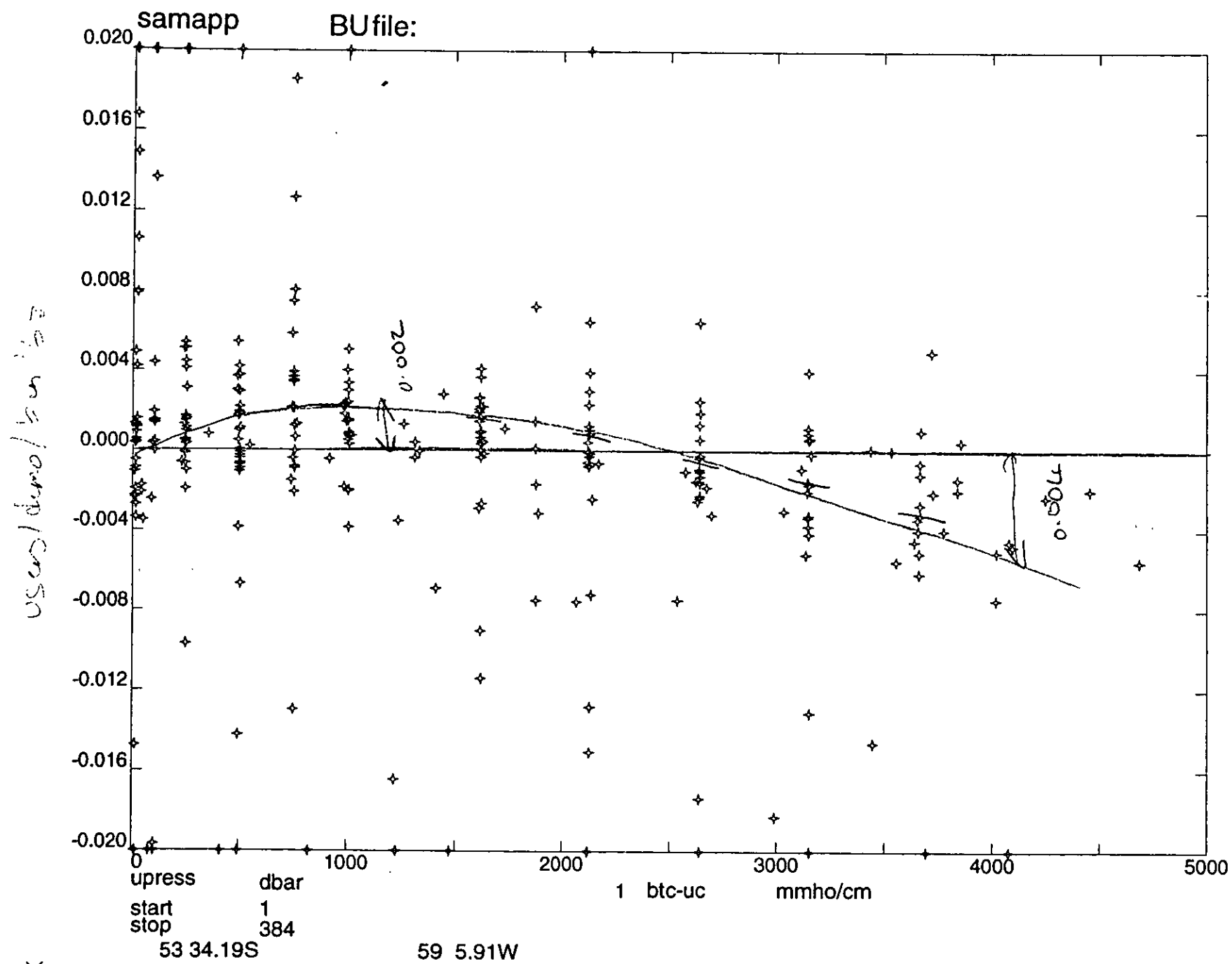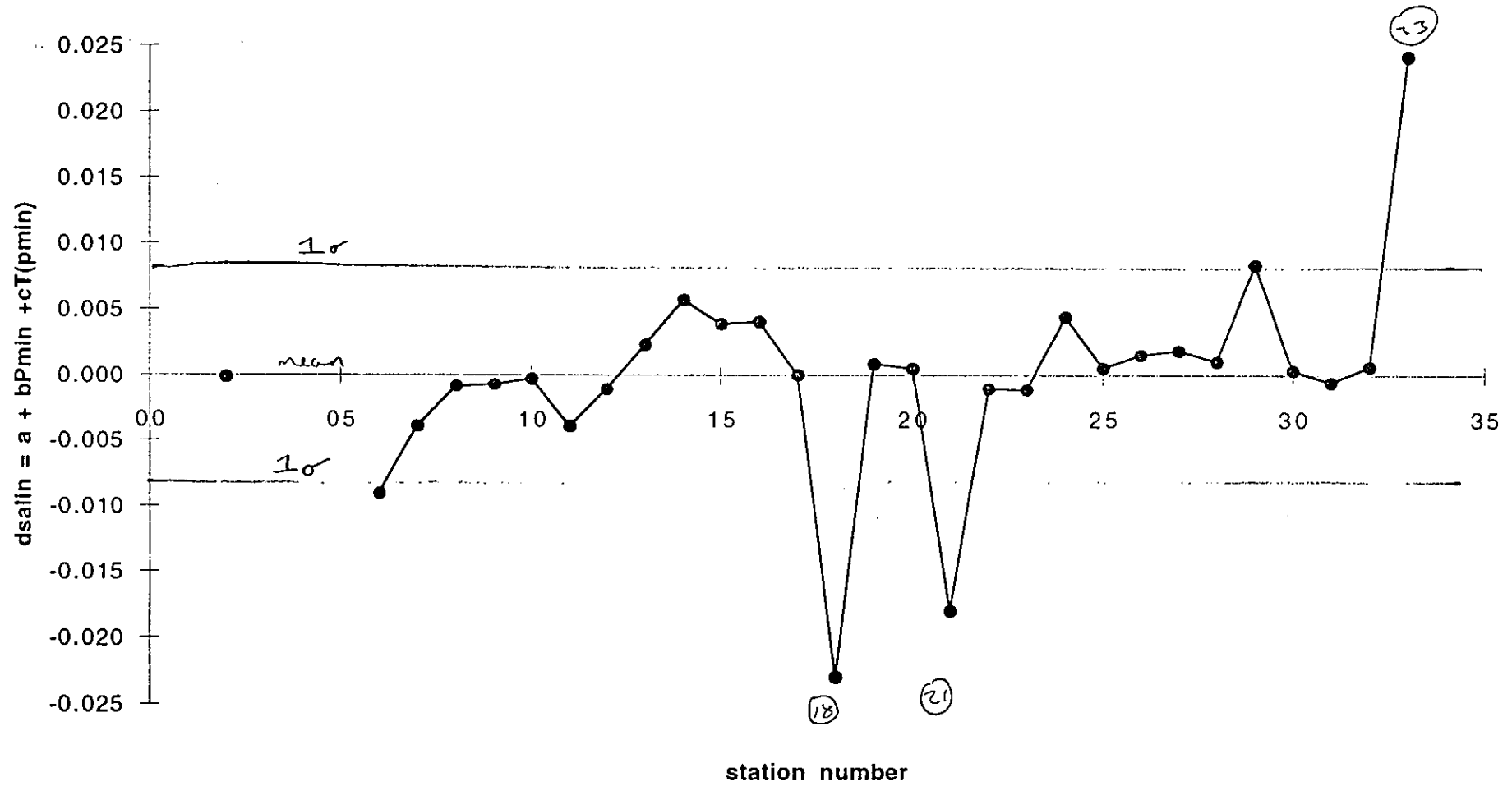
Figure 7a

dsalin at Pmax

Figure 7.b

Figure 8 a)

samapp   AB file:

upress   dbar
start   1
stop   348
53 34.19S   59 5.91W

1   bts-us   pss-78
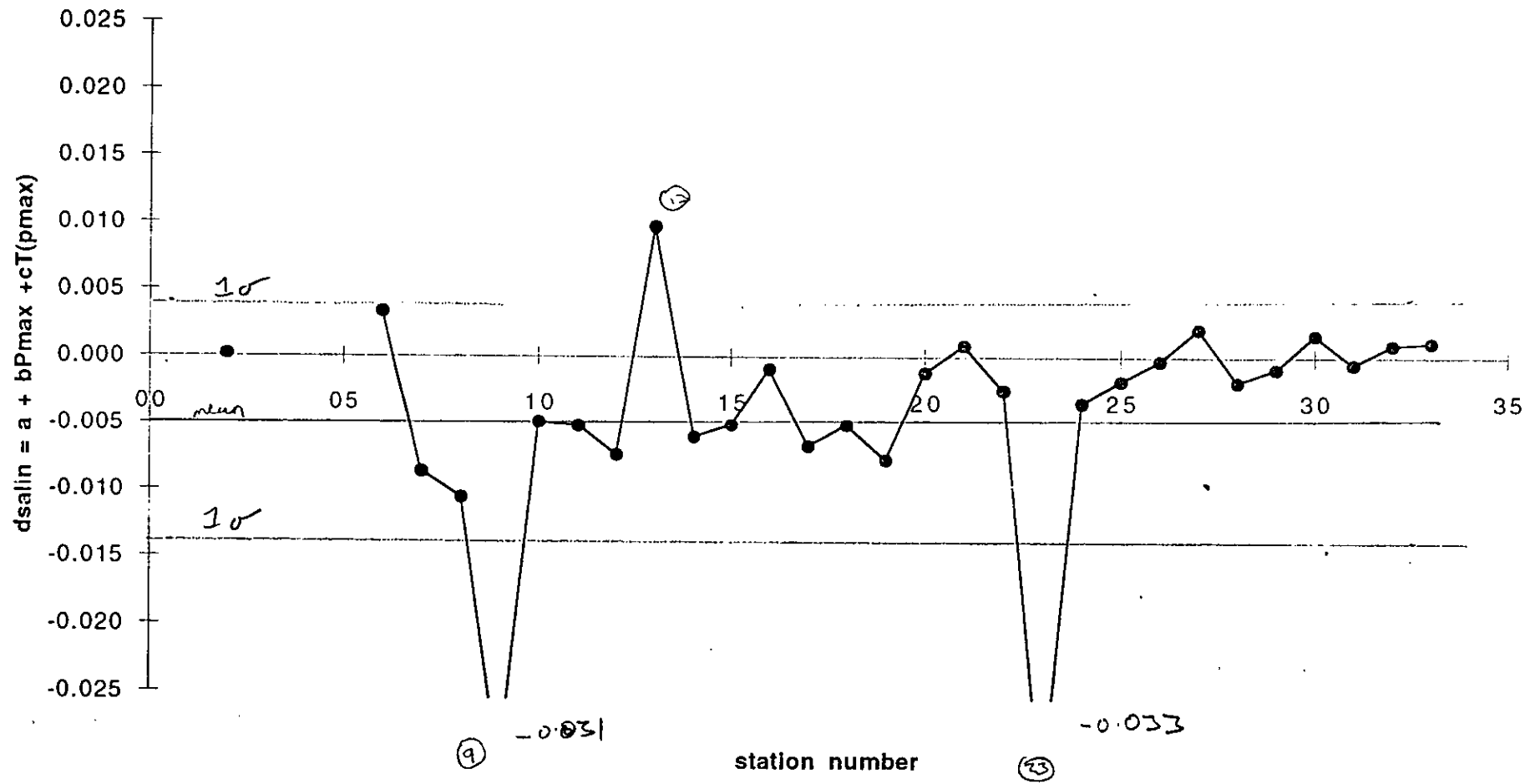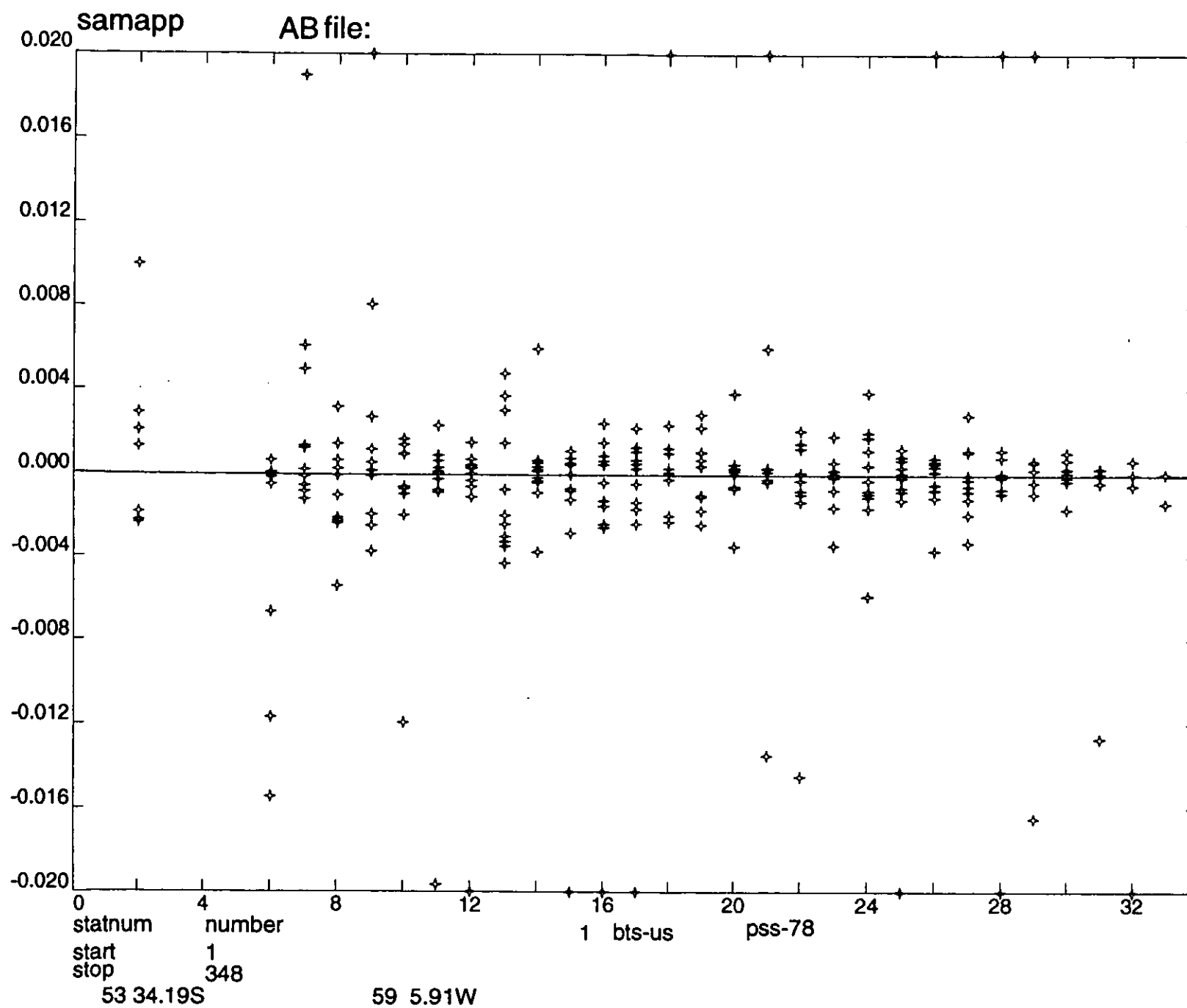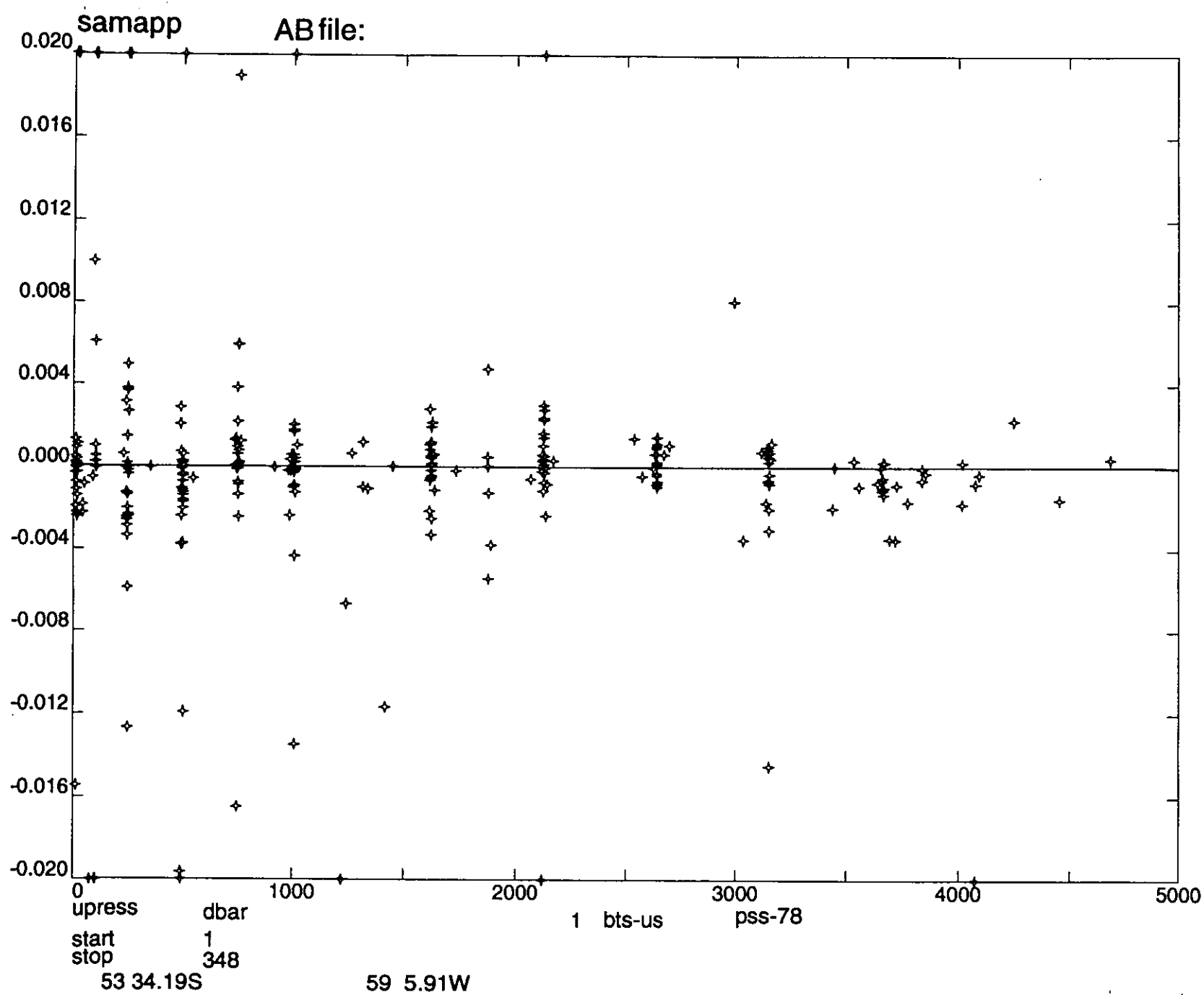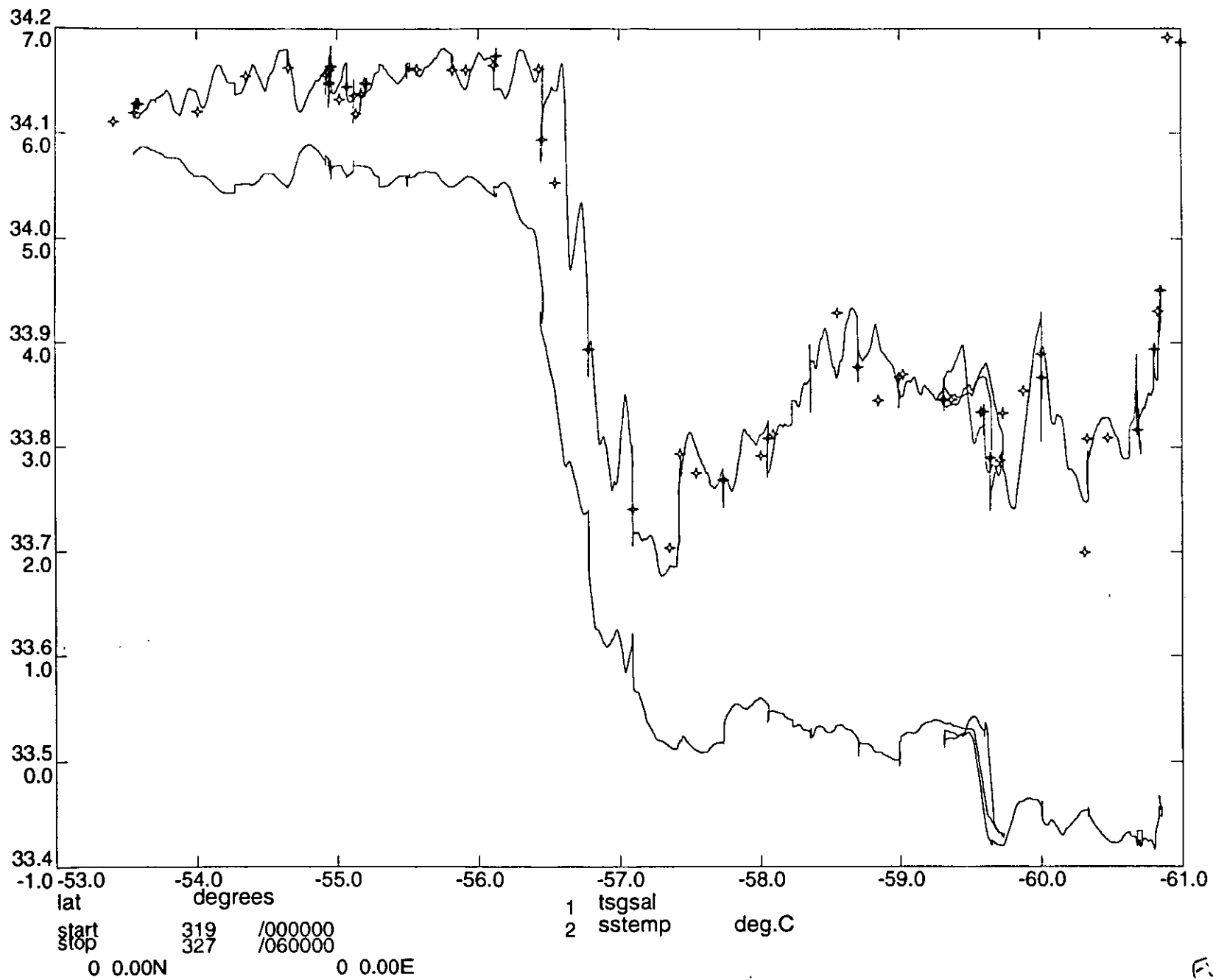
Figure 8b

Figure 9

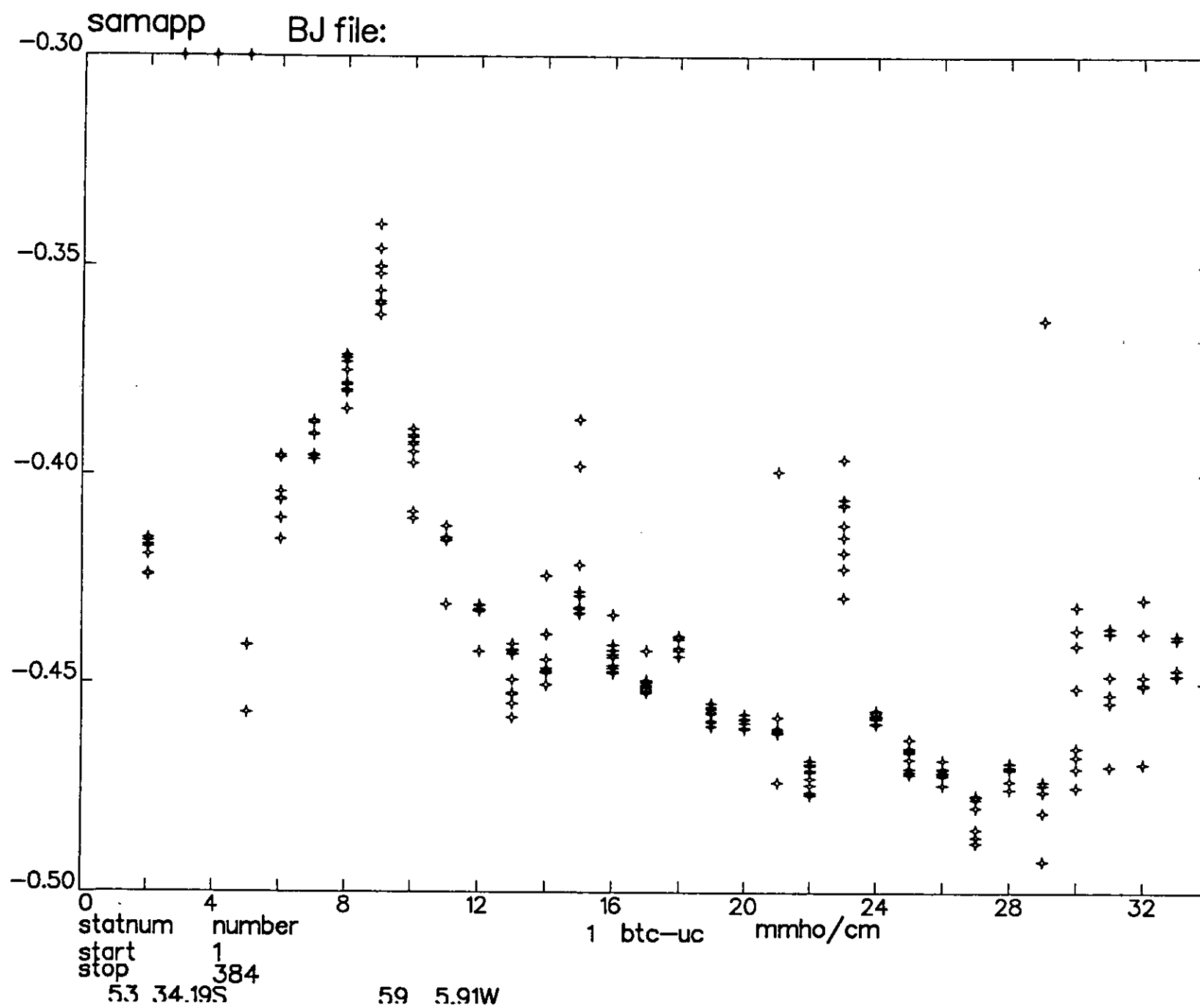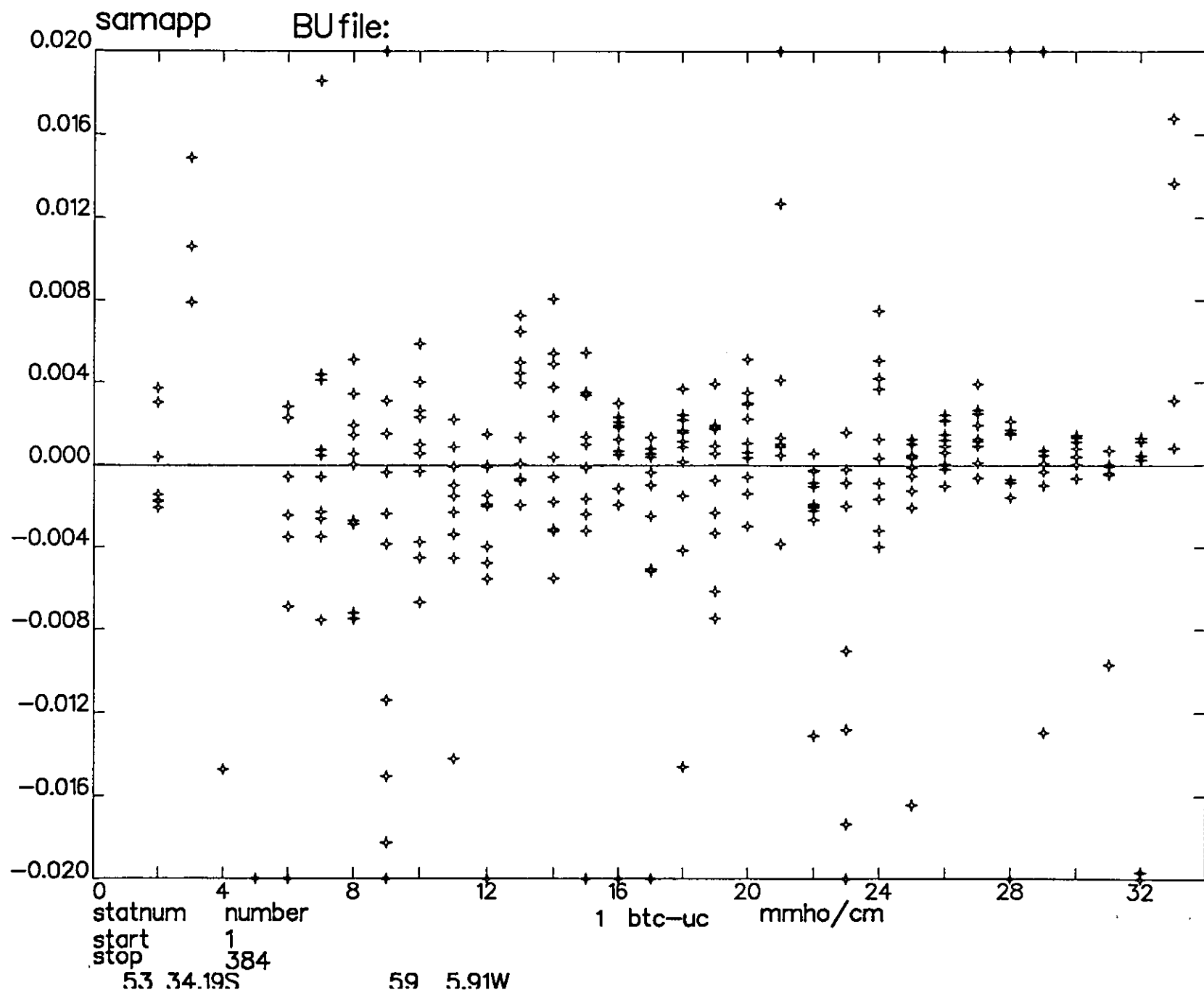| Stn no.	Cast no.	Date yymmdd	start GMT	bottom GMT	end GMT	latitude degrees S	longitude degrees W	Depths incdepth m	orrdepth m	tarea	ht. off m	wire m	max P dbar	Samples no.	notes
01	1	941115	054930	061000	063500	-53 34.70	-59 6.38	1910.5	1881.9	36	n/a	1256	n/a	0	test cast. aborted
02	1	941115	190135	092540	101214	-53 34.19	-59 5.91	1898.7	1870.2	36	n/a	n/a	1711	8	test cast
03	1	941115	163129	164742	170451	-54 39.08	-58 33.61	209.2	205.6	36	24	180	183	3	start section - cond bad
04	1	941115	190135	192012	194600	-54 55.49	-58 21.63	670.6	657.7	36	30	640	651	1	cond bad
05	1	941115	222541	225333	233007	-54 57.58	-58 23.00	1464.7	1440.6	36	n/a	1440	1473	9	cond bad
06	1	941116	032058	040655	045453	-54 57.36	-58 21.55	1508.8	1484.2	36	15	1440	1453	9	cond OK
07	1	941116	113154	120935	131200	-55 4.15	-58 17.25	2083.1	2053.6	36	20	2026	2069	10	
08	1	941116	140149	144636	155315	-55 7.29	-58 15.41	2546.0	2514.5	36	20	2470	2535	11	
09	1	941116	164521	173729	190300	-55 10.30	-58 14.82	3025.3	2993.8	36	60	2898	2991	10	
10	1	941116	194501	204701	220745	-55 12.82	-58 13.55	3765.6	3739.8	36	180	3552	3641	10	
11	1	941117	003955	015645	033400	-55 31.24	-58 0.31	4246.1	4227.1	36	n/a	n/a	4247	10	
12	1	941117	061740	073950	092509	-55 49.11	-57 52.26	4627.9	4615.9	36	10	4563	4691	11	
13	1	941117	113233	123626	140620	-56 7.72	-57 40.26	3736.2	3701.1	33	20	3660	3717	11	
14	1	941117	164444	174542	193300	-56 27.33	-57 29.55	3579.6	3542.9	33	50	3531	3555	11	
15	1	941117	214823	223729	235125	-56 47.14	-57 18.27	2598.2	2559.7	33	n/a	2650	2699	10	
16	1	941118	030358	042301	060109	-57 5.58	-57 7.21	4423.9	4398.9	33	40	4350	4455	11	
17	1	941118	084349	095317	112609	-57 25.73	-56 55.66	4006.7	3974.2	33	20	3919	4017	11	
18	1	941118	134740	144820	163400	-57 44.10	-56 42.11	3418.9	3381.4	33	n/a	3392	3447	11	
19	1	941118	184322	195946	213813	-58 3.42	-56 32.95	3979.7	3940.0	34	65	n/a	4015	11	
20	1	941119	002005	012607	030900	-58 21.68	-56 20.86	3863.1	3822.2	34	50	3739	3837	11	
21	1	941119	061400	072334	090512	-58 41.62	-56 9.53	3839.4	3798.3	34	20	3750	3853	11	
22	1	941119	112219	122530	135300	-58 59.76	-55 57.88	3820.3	3779.0	34	15	3730	3837	11	
23	1	941119	222728	233905	011900	-59 35.79	-55 51.95	3707.3	3664.8	34	40	3597	3693	11	west of section
24	1	941120	033222	043549	060229	-59 18.68	-55 42.04	3774.6	3732.8	34	35	3660	3771	11	
25	1	941120	083422	093805	112000	-59 38.81	-55 30.96	3724.8	3682.6	34	26	3625	3723	11	
26	1	941120	134515	144314	160712	-60 0.29	-55 19.66	3548.2	3504.7	34	40	3434	3533	11	
27	1	941120	183831	193533	205250	-60 20.16	-55 4.80	3481.7	3438.2	34	60	3340	3437	11	
28	1	941121	034213	043817	055752	-60 40.86	-54 48.72	3145.2	3100.7	34	28	3033	3115	10	
29	1	941121	070525	075149	085909	-60 48.05	-54 43.12	2597.4	2553.9	34	15	2505	2571	10	
30	1	941121	122044	125047	134851	-60 49.80	-54 43.04	1699.7	1664.2	34	40	1679	1729	8	
31	1	941121	144438	150043	152919	-60 51.12	-54 42.72	951.2	927.7	34	30	896	919	6	
32	1	941121	164145	165158	171122	-60 58.92	-54 37.34	604.5	587.9	34	46	536	551	6	
33	1	941121	181756	182539	184819	-61 3.01	-54 36.02	396.1	381.7	32	15	351	357	4	end section

Table 1

Year	A	SE	B	SE	N	R2	COV
1993	-596.074	0.005	17.19	0.27	70	0.984	4.84E-03
1994	-559.272	0.006	16.13	0.38	40	0.977	4.42E-03

SE is the standard error, N is the sample number, R2 correlation coefficient and COV the covariance

Table 2

P dbar	dp(5500(P) dbar
5500	0.0
5000	0.9
4500	1.7
4000	2.5
3500	3.2
3000	4.1
2500	5.1
2000	6.0
1500	6.7
1000	6.5
500	3.3
300	2.7
100	0.6
0	0.0

Table 3

STN	A	B	Rsq	A2	B2	Rsq
01	n/a	n/a	n/a	n/a	n/a	n/a
02	-2.14E-02	1.17E-05	0.890	-2.12E-02	1.17E-05	0.891
03	-1.58E-01	1.23E-03	0.985	-1.46E-01	1.14E-03	1.000
04	-1.01E-01	8.96E-05	0.086	-1.01E-01	8.96E-05	0.086
05	-1.95E-01	1.36E-04	0.790	-1.95E-01	1.36E-04	0.790
06	-4.71E-02	3.11E-05	0.976	-4.77E-02	3.15E-05	0.976
07	-4.73E-02	2.13E-05	0.943	-4.70E-02	2.11E-05	0.943
08	-4.58E-02	1.70E-05	0.938	-4.52E-02	1.68E-05	0.938
09	-6.64E-02	2.05E-05	0.977	-6.57E-02	2.03E-05	0.977
10	-4.29E-02	1.10E-05	0.976	-4.21E-02	1.08E-05	0.976
11	-3.59E-02	8.01E-06	0.978	-3.55E-02	7.93E-06	0.978
12	-2.67E-02	5.28E-06	0.967	-2.63E-02	5.20E-06	0.967
13	-2.90E-02	7.10E-06	0.923	-2.85E-02	6.99E-06	0.923
14	-3.13E-02	8.05E-06	0.961	-3.07E-02	7.90E-06	0.961
15	-3.28E-02	1.11E-05	0.979	-3.20E-02	1.08E-05	0.979
16	-1.91E-02	4.06E-06	0.968	-1.87E-02	3.97E-06	0.968
17	-1.72E-02	4.09E-06	0.944	-1.69E-02	4.01E-06	0.944
18	-3.57E-02	5.73E-06	0.941	-3.49E-02	5.61E-06	0.942
19	-2.35E-02	5.66E-06	0.927	-2.29E-02	5.53E-06	0.927
20	-1.37E-02	3.46E-06	0.682	-1.35E-02	3.39E-06	0.682
21	-1.35E-02	3.38E-06	0.266	-1.32E-02	3.31E-06	0.267
22	-1.09E-02	2.64E-06	0.886	-1.06E-02	2.58E-06	0.886
23	-6.24E-02	1.67E-05	0.971	-6.13E-02	1.64E-05	0.971
24	-2.02E-02	5.08E-06	0.914	-1.96E-02	4.95E-06	0.914
25	-1.39E-02	3.50E-06	0.806	-1.36E-02	3.42E-06	0.806
26	-1.01E-02	2.67E-06	0.890	-9.80E-03	2.60E-06	0.891
27	-1.35E-02	3.83E-06	0.768	-1.32E-02	3.75E-06	0.768
28	-1.83E-02	5.49E-06	0.755	-1.79E-02	5.36E-06	0.755
29	-8.33E-03	3.18E-06	0.606	-8.21E-03	3.14E-06	0.606
30	-1.04E-02	4.37E-06	0.358	-1.01E-02	4.28E-06	0.358
31	-2.73E-03	2.64E-06	0.210	-2.67E-03	2.57E-06	0.209
32	-2.00E-02	3.52E-05	0.877	-1.93E-02	3.41E-05	0.878
33	-6.32E-03	1.69E-05	0.015	-3.12E-02	8.99E-05	0.815

Table 4

STN	A	B	R2
01*	0.0000	1.0000	n/a
02	-0.2057	0.9935	0.920
03*	0.0000	1.0000	n/a
04*	0.0000	1.0000	n/a
05*	0.0000	1.0000	n/a
06	-0.8564	1.0140	0.797
07	-0.2723	0.9964	0.396
08	-0.0173	0.9889	0.865
09	-0.0502	0.9909	0.832
10	0.1109	0.9842	0.863
11	-0.1533	0.9918	0.867
12	-0.0675	0.9886	0.965
13	0.0030	0.9859	0.922
14	0.0668	0.9838	0.774
15	0.2399	0.9787	0.970
16	0.1499	0.9810	0.982
17	0.1215	0.9817	0.994
18	0.1749	0.9802	0.982
19	0.1616	0.9801	0.942
20	0.0709	0.9828	0.958
21	0.0909	0.9820	0.866
22	0.1108	0.9812	0.994
23	0.1073	0.9834	0.992
24	0.2778	0.9761	0.943
25	0.1183	0.9810	0.997
26	0.2632	0.9759	0.996
27	0.1238	0.9803	0.994
28	0.1331	0.9802	0.964
29	-0.1556	0.9895	0.944
30	0.0720	0.9820	0.998
31	0.1041	0.9808	0.999
32	0.4559	0.9687	0.997
33	0.2726	0.9749	0.933

Table 5

STN	A	B	C	Pmin	T(pmin)	Pmax	T(pmax)	dsalin Pmin	dsalin Pmax
02	137.16	-0.0520	-25.90	42.4	5.205	985.8	3.325	0.000	0.000
03									
04									
05									
06	-51.23	0.0146	10.65	12.9	5.645	1447.0	2.511	-0.009	
07	-48.57	0.0178	9.45	10.9	5.540	2066.2	2.155	-0.004	-0.009
08	-39.15	0.0145	7.06	15.6	5.638	2534.8	1.837	-0.001	-0.011
09	-29.54	0.0176	5.29	10.8	5.691	2989.5	1.439	-0.001	-0.031
10	-30.77	0.0086	5.49	14.5	5.639	3637.3	0.767	0.000	-0.005
11	-24.92	0.0069	5.19	15.5	5.549	4246.0	0.164	-0.004	-0.005
12	-15.45	0.0047	3.01	13.8	5.466	4687.5	0.189	-0.001	-0.007
13	7.28	-0.0042	-1.75	12.1	5.451	3716.3	0.711	0.002	0.010
14	-9.58	0.0042	0.93	14.2	4.104	3554.0	0.541	0.006	-0.006
15	1.15	0.0027	-3.49	77.7	1.508	2696.7	0.973	0.004	-0.005
16	-4.58	0.0012	0.53	16.5	0.971	4454.4	0.028	0.004	-0.001
17	0.15	0.0016	-0.91	10.7	0.198	4016.2	-0.094	0.000	-0.007
18	22.63	-0.0054	-11.12	20.0	-0.038	3445.6	-0.081	-0.023	-0.005
19	-0.77	0.0020	-1.80	16.6	0.076	4014.3	-0.268	0.001	-0.008
20	-0.18	0.0002	-2.64	11.3	0.119	3835.9	-0.225	0.000	-0.001
21	15.79	-0.0055	-12.11	14.3	-0.187	3852.2	-0.366	-0.018	0.001
22	1.08	0.0004	-0.06	9.7	0.121	3836.2	-0.330	-0.001	-0.002
23	2.26	0.0079	-4.47	13.8	0.274	3690.5	-0.359	-0.001	-0.033
24	-4.05	0.0018	-1.73	19.8	0.223	3771.6	-0.353	0.004	-0.003
25	-0.79	0.0007	-0.30	17.0	-0.738	3722.7	-0.367	0.001	-0.002
26	-2.02	0.0006	-1.15	16.6	-0.401	3532.2	-0.348	0.002	0.000
27	-2.03	0.0000	-0.25	18.4	-0.668	3436.6	-0.268	0.002	0.002
28	-2.10	0.0012	-1.18	15.9	-0.902	3115.5	-0.332	0.001	-0.002
29	-5.85	0.0027	2.80	11.2	-0.890	2571.2	-0.097	0.008	-0.001
30	0.08	-0.0011	0.90	12.1	-0.439	1727.3	0.110	0.000	0.002
31	2.16	-0.0022	1.99	14.1	-0.780	918.7	0.195	-0.001	-0.001
32	-12.36	0.0061	-14.73	102.1	-0.755	550.0	-0.552	0.001	0.001
33	49.48	0.0765	106.60	17.1	-0.703	356.6	-0.730	0.024	0.001
							mean	0.000	-0.005
							stdev	0.008	0.009

Table 6

PoR	RTM	A	B	DoC	SRC
1	T714	1.51E-02	1.000879	7/6/94	IOSDL
3	T401	-1.93E-02	1.000635	7/6/94	IOSDL
3	T746	-5.11E-03	1.000502	7/6/94	IOSDL

Table 7

Pair	N	mean	sd	N(<2sd)	mean	sd
T714-CTD	32	0.1913	0.9993	23	-0.0051	0.0021
T401-CTD	29	0.0118	0.3681	29	-0.0044	0.0014
T746-CTD	30	0.0148	0.3659	20	-0.0029	0.0013
				mean =	-0.0041	

Table 8

XBT Probe Type Number		Day Number	Time GMT	Lat		Lon		PES Depth	Surface Temp.
				degrees	minutes	degrees	minutes		
	T7	322	0625	-57	6.6	-57	3.7	4335	
839095	T7	322	0743	-57	17.4	-56	58.1	4069	0.2
	T7	322	1232	-57	36.6	-56	47.3	3211	
839097	T7	322	1241	-57	37.8	-56	46.4	3418	0.1
839096	T7	323	0439	-58	32.4	-56	13.8	3848	0.3
839104	T7	323	1500	-59	9.6	-55	48.9	3713	0.4
	T7	324	0207	-59	27.7	-55	45.9		0.3
	T7	324	0725	-59	30.0	-55	35.0	3749	
	T7	324	0731	-59	30.6	-55	34.6	3747	
	T7	324	1204	-59	47.4	-55	25.0	3678	
	T7	324	1222	-59	49.8	-55	23.7	3635	-0.4

Table 9

Average speed and heading corrections

Number in average	Ratio of GPS to ADCP speed	GPS direction	ADCP direction	GPS-ADCP direction difference (allowing for 180° ambiguity)
15	0.988	-105.540	72.210	2.250
15	0.996	-106.132	71.513	2.354
14	1.013	-105.677	71.347	2.976
15	1.004	-105.832	71.529	2.639
15	1.000	-106.254	71.292	2.454
15	0.992	-106.644	71.273	2.083
15	0.996	127.724	-54.086	1.810
15	1.002	126.705	-55.711	2.415
13	1.006	-170.334	7.579	2.088
12	1.005	178.760	-2.948	1.708
11	1.018	-91.780	86.277	1.942
15	0.994	-93.168	84.420	2.412
11	0.993	-109.633	67.920	2.447
15	1.001	-110.748	67.136	2.117
15	0.992	-110.710	66.911	2.378
14	0.994	-110.603	67.217	2.181
15	0.995	-112.004	65.563	2.433
15	0.998	-76.496	101.440	2.064
10	0.996	-76.250	101.818	1.932
14	1.004	-75.793	102.256	1.951
14	0.989	-75.396	102.656	1.948
15	0.996	-73.242	104.612	2.146
14	0.995	-72.242	106.022	1.737
12	1.006	-70.951	106.981	2.068
15	0.984	-67.090	110.969	1.941
13	0.998	-69.277	108.694	2.029
11	1.016	43.607	-138.118	1.724
11	1.004	-138.289	39.473	2.239
15	1.007	-112.958	65.451	1.591
13	1.002	-134.130	43.693	2.178